ChemPubSoc Europe

DOI: 10.1002/cphc.201701363

CHEMPHYSCHEM Minireviews

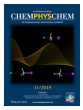

Nucleophilic Substitution (S_N2): Dependence on Nucleophile, Leaving Group, Central Atom, Substituents, and Solvent

Trevor A. Hamlin,[a] Marcel Swart,*[a, b] and F. Matthias Bickelhaupt*[a, c]

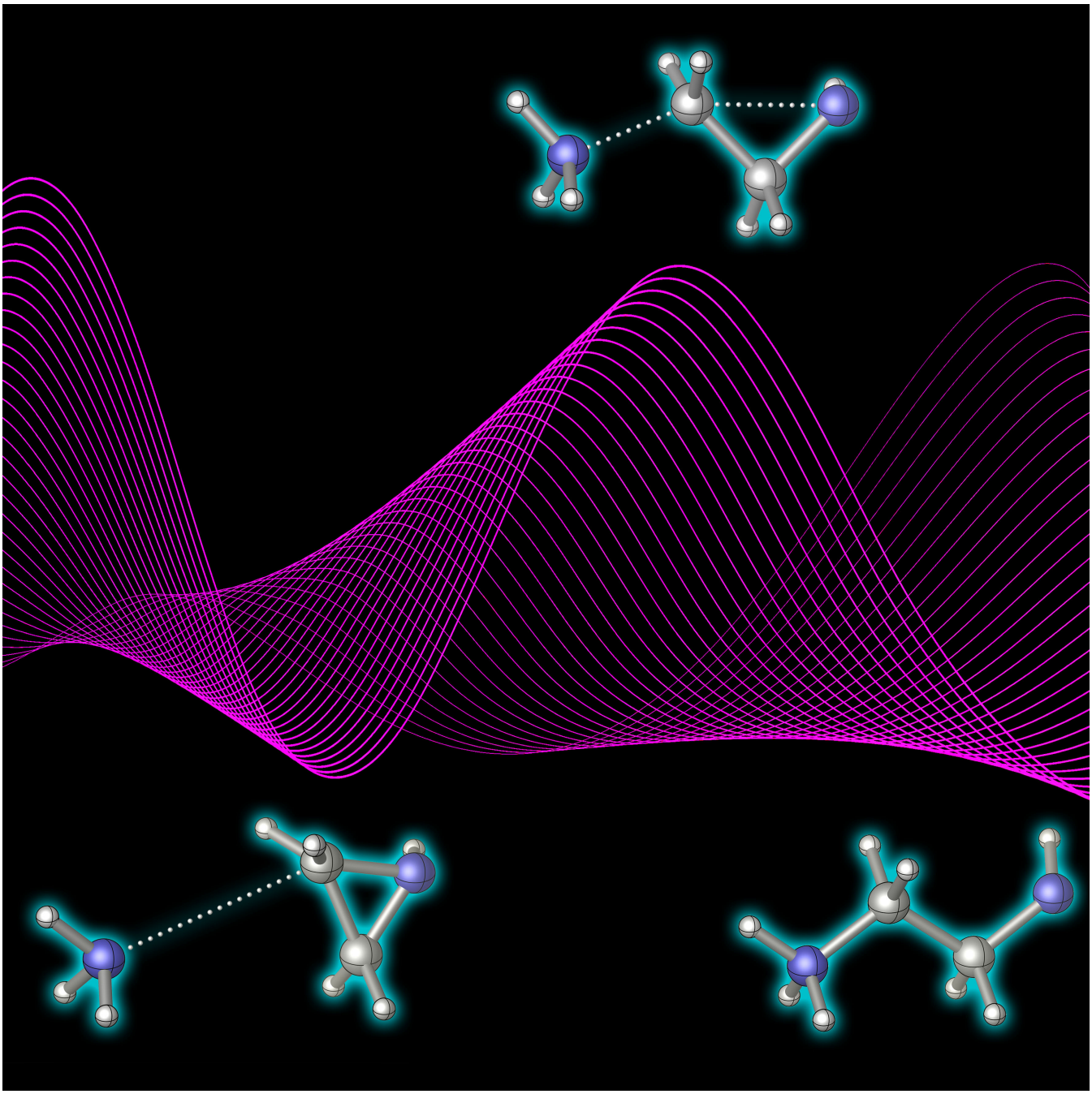

Abstract: The reaction potential energy surface (PES), and thus the mechanism of bimolecular nucleophilic substitution (S_N2), depends profoundly on the nature of the nucleophile and leaving group, but also on the central, electrophilic atom, its substituents, as well as on the medium in which the reaction takes place. Here, we provide an overview of recent studies and demonstrate how changes in any one of the aforementioned factors affect the S_N2 mechanism. One of the most striking effects is the transition from a double-well to a single-well PES when the central atom is changed from a second-period (e.g. carbon) to a higher-period element (e.g, silicon, germanium). Variations in nucleophilicity, leaving group ability, and bulky substituents around a second-row element central atom can then be exploited to change the single-well PES back into a double-well. Reversely, these variations can also be used to produce a single-well PES for second-period elements, for example, a stable pentavalent carbon species.

1. Introduction

Bimolecular nucleophilic substitution (S_N2) reactions constitute one of the most widely-used organic chemistry reactions, both in chemistry and biology.[1] The general reaction scheme is summarized in Scheme 1, where a nucleophile Nu^q attacks the central atom A and simultaneously a leaving group LG is displaced. The reaction can proceed for either anionic species (typically $q1 = q4 < 0$), neutral (radical) species (typically $q1 = q2 = q3 + q4 = 0$), or cationic species (typically $q2 = q3 > 0$), together with a wide range of nucleophiles, leaving groups and central atoms. The number and nature of the substituents around the central atom play a major role in determining reactivity.

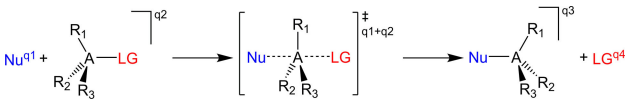

Scheme 1. General reaction scheme for S_N2 reactions, where Nu is the nucleophile, A the central atom, and LG the leaving group (q1–q4 is the charge of the respective species: $q1 + q2 = q3 + q4$).

The archetypal S_N2 reaction is characterized by a chloride anion ($Nu = Cl^-$) attacking methyl chloride ($A = C$, $LG = Cl^-$) and is accompanied by a double-well potential energy surface (PES) (see Scheme 2). Starting from the reactants R, the profile shows a reactant complex RC in which the nucleophile forms an encounter complex (sometimes referred to as an ion-dipole complex) with the substrate that is stabilized by both electrostatic and donor-acceptor orbital interactions. After proceeding over the barrier of the transition state TS, a similar product complex PC is formed where the leaving group is still weakly bound to the substrate. Finally, the products P are obtained. The surface contains two distinct barriers, the central barrier $\Delta E^{\ddagger,centr}$ that relates the TS to the reactant complex RC (which is always positive), and an overall barrier $\Delta E^{\ddagger,ovr}$ that relates the TS to the separated reactants and which can, in principle, have a negative value (for gas-phase anionic S_N2 reactions, it indeed often is).

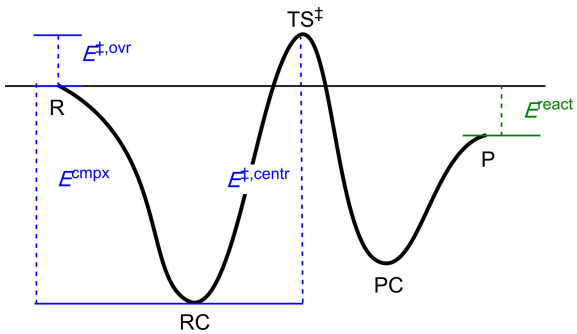

Scheme 2. Energy profile for a typical S_N2 reaction, going from reactants R to reactant complex RC, transition state TS, product complex PC, and products P.

S_N2 substitution is, in principle, always in competition with base-induced elimination (E2), and the two pathways may occur as unwanted side reactions of each other (see Scheme 3).[2]

A number of computational benchmark studies have been performed to assess various S_N2 reactions and/or the S_N2/E2 competition by our group[3] as well as others.[4] Furthermore, the substitution may take place via either simultaneous breaking and forming of the bonds involved (S_N2), or via a mechanism where the breaking of the old bond precedes the formation of the new bond (S_N1). A clear-cut distinction between these two may not always be possible.[5] It was argued

[a] *Dr. T. A. Hamlin, Prof. Dr. M. Swart, Prof. Dr. F. M. Bickelhaupt*
Department of Theoretical Chemistry and
Amsterdam Center for Multiscale Modeling (ACMM),
Vrije Universiteit Amsterdam,
De Boelelaan 1083, 1081 HV Amsterdam, (The Netherlands)
E-mail: f.m.bickelhaupt@vu.nl
[b] *Prof. Dr. M. Swart*
Institut de Química Computacional I Catàlisi and Department de Química,
Universitat de Girona, 17003 Girona, Spain
and
ICREA, Pg. Lluís Companys 23, 08010 Barcelona, (Spain)
E-mail: marcel.swart@udg.edu
[c] *Prof. Dr. F. M. Bickelhaupt*
Institute of Molecules and Materials (IMM)
Radboud University
Heyendaalseweg 135, 6525 AJ Nijmegen (The Netherlands)

that aliphatic nucleophilic substitutions occur by the stepwise S_N1 mechanism when the carbocation intermediate exists in an energy well for at least the time of a bond vibration ($\approx 10^{-13}$ s). The change to the S_N2 mechanism would then be "enforced" when the energy well for the intermediate disappears. Mayr and co-workers used this working hypothesis to propose a formula that relates the reaction rate k to a carbocation-specific electrophilicity parameter E, and solvent-dependent nucleophile specific parameters s and N: $k = s\,(N + E)$.[5]

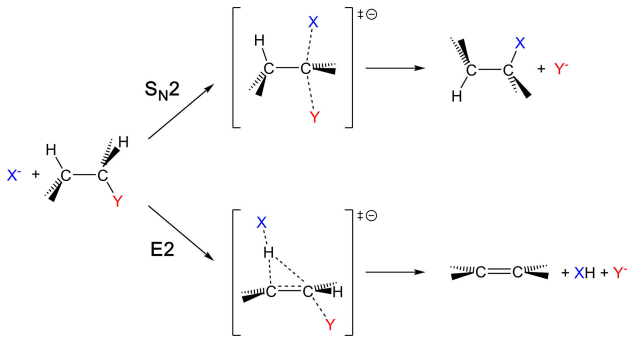

Scheme 3. A general representation of the competition between S_N2 and E2 mechanisms.

Rablen and co-workers[6] explained and quantified the effects of alkyl halide structure on S_N2 and E2 barriers at the high-level G4 method. Employing CN^- as a nucleophile and Cl^- as a leaving group, they investigated substitution patterns on the alkyl halide, including α- and β-methylation, adjacent unsaturated functional groups (allyl, benzyl, propargyl, α to carbonyl), ring size, and α-halogenation and cyanation. The work showcased the underappreciated fact that E2 reactions are just as sensitive to structural variations as their S_N2 counterparts.

Wolters et al. studied[7] the effect of acidic and basic conditions on the competition between the elimination and substitution pathways for two related model systems, namely, $H_2O + C_2H_5OH_2^+$ (acidic, see Scheme 1: q1 = 0, q2 = +1) and $OH^- + C_2H_5OH$ (basic, see Scheme 1: q1 = −1, q2 = 0). It was found that under acidic conditions the substitution pathway was preferred, whereas the elimination pathway prevails under basic conditions. The divergent reactivity, depending on the pH, was rationalized by means of the activation strain model (ASM) and quantitative molecular orbital (MO) theory.[8] The activation strain model is a useful tool for analyzing activation barriers, which are the sum of the energies required to distort the reactants into geometries they have in the transition state, as well as the interaction energies between the deformed reactants. The barriers for either substitution or elimination in the acidic case were very similar, with the former case being preferred by only 3.1 kcal/mol. Analysis revealed that the elimination pathway predominates under basic conditions due to the increased basicity of the nucleophile, which leads to a more stabilizing interaction energy originating from the enhanced HOMO (OH^-)-LUMO (substrate) orbital interactions. The shift in preference towards the elimination pathway under basic conditions is furthermore caused by a fundamental change in LUMO composition, which becomes C^β–H antibonding in basic conditions (thus promoting β-proton abstraction by

Trevor A. Hamlin studied Biochemistry at Albright College where he obtained his B.S. in 2010 (cum laude) with an ACS certification and carried out undergraduate research under the tutelage of Christian S. Hamann and Dean J. Tantillo (UC Davis). In 2015, he earned his Ph.D. in Chemistry at The University of Connecticut under the supervision of Nicholas E. Leadbeater, where he employed a joint experimental/theoretical approach toward the development of new oxidation protocols involving green and recyclable oxoammonium salts. He joined the Theoretical Chemistry Department at Vrije Universiteit Amsterdam in 2015 for a postdoctoral position. His research interests involve the computational modeling of organic, inorganic, and biochemical reactions with a special interest in predicting and understanding molecular reactivity.

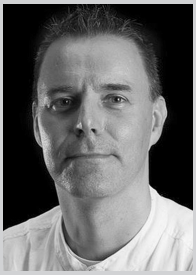

Marcel Swart obtained his Ph.D. at the University of Groningen with a study on copper proteins in 2002. He joined the IQCC (University of Girona) in 2006 and was soon after promoted to ICREA Research Professor in 2009. He was awarded the Young Scientist Excellence Award 2005, the MGMS Silver Jubilee Prize 2012, was elected for the Young Academy of Europe (2014) and its Board (2016), and elected a fellow of the Royal Society of Chemistry in 2015. He works in the field of theoretical (bio) inorganic and supramolecular chemistry, with a focus on transition-metal complexes, metalloproteins, enzymes, and DNA.

Matthias Bickelhaupt holds Chairs in Theoretical Chemistry at Vrije Universiteit Amsterdam and Radboud University Nijmegen. He received his Ph.D. at the University of Amsterdam with Nico Nibbering and Evert Jan Baerends in 1993, in the fields of Mass Spectrometry and Theoretical Chemistry. Afterwards, he worked with Paul v. R. Schleyer, Tom Ziegler and Roald Hoffmann, became assistant professor in Marburg, and obtained tenure in Amsterdam in 1999. He has published on developments in the analysis and theory of the chemical bond as well as chemical reactivity, with applications in organic, inorganic, and biological chemistry. He is a member of the Royal Holland Society for Sciences and Humanities and received the VICI award (2002) of the Netherlands Organization for Scientific Research.

a Lewis base) whereas it has C^{β}–H bonding character (which stabilizes this bond upon interaction with a Lewis base) under acidic conditions, i.e., after protonation.

Solvent effects have a large influence on the reactivity and mechanism of S_N2 reactions.[9] This is, in particular, true for ionic S_N2, where the degree of charge (de) localization determines the enhanced stability. For instance, the solvation energy is much more favorable for reactants where the charge is located at the nucleophile, e.g. Cl^-. Instead, in the transition state, the total (negative) charge is delocalized over the nucleophile, central atom and leaving group with a concomitant reduction of the solvation energy. As a result, the energy profile changes from a double-well PES into a unimodal one for ionic S_N2 reactions,[9b] with a substantial increase of the barrier and hence the reactions are much slower in solution than in the gas-phase. A noteworthy exception involves S_N2 reactions between uncharged reactants, e.g., the Menshutkin reaction,[10] where a decrease in the energy barrier is observed as solvent polarity is increased (See Scheme 1, q1 = q2 = 0, q3 = +1, q4 = −1).[11] The rate enhancement in polar solvents is due to stabilization of charge separation in the transition state.

Microsolvation studies have been important for establishing the effect of gradual solvation on S_N2 reactivity. Bohme and co-workers demonstrated the drastic decrease in reaction rates of S_N2 reactions as the size of the water cluster around the nucleophile increased.[12] Some years later, these experimental observations were validated computationally.[13] Recent studies probing the effects of microsolvation by means of chemical dynamics simulations have found that there may not be equilibrium solvation throughout the course of the S_N2 reaction.[14] Additionally, these studies propose that the encounter complex is strongly favored, leading to a preference for an indirect S_N2 mechanism, like the one pictured in Scheme 2, over the direct attack by a nucleophile.[15] Microsolvation effects have been investigated for other nucleophiles, including, F^-,[15b] Cl^-,[16] OH^-,[17] and HOO^-.[18]

Hamlin et. al. recently studied the effect of various polar and apolar solvents on the shape of the PES for identity S_N2@C, S_N2@Si, S_N2@P, and S_N2@As reactions.[19] They demonstrated the relationship between solvation energy and charge localization. A higher localization of charge leads to greater stabilization by the solvent. The degree of charge transfer from the HOMO of the nucleophile to the substrate is strongly related to the size of the LUMO of the central atom. Smaller LUMO's, on the electrophilic C and P, lead to an abrupt charge transfer near the transition complex, which is associated with increased solvation energies (due to charge localization on the nucleophile). This, in turn, results in large changes in PES depending on the polarity of the solvent. Central atoms with a large LUMO (Si and As) lead to a more gradual transfer of charge and thus a decreased solvation energy, which results in PES curvature that is more resistant to solvent effects.

Significant progress has been made towards understanding the atomistic dynamics underpinning gas-phase S_N2 reactions. Hase and coworkers have made an enormous impact on the field: their seminal studies involved classical dynamics simulations of the archetypal $Cl^- + CH_3Cl$ reaction. They determined that the S_N2 reaction was not significantly promoted by vibrational energy, but instead found a strong coupling between the rotational degrees of freedom and translation.[20] The gas-phase $Cl^- + CH_3Br$ and $Cl^- + CD_3Br$ reactions were probed using elegant kinetic studies by Viggiano et. al. and their conclusions were fully consistent with the previous findings by Hase.[21] The encounter complex, that is a common stationary point on the PES, can be avoided completely during a direct mechanism promoted by $X^- + CH_3Y$ relative translational or CH_3Y vibrational excitations.[20b,22] Wester and co-workers investigated the dynamics of other simple S_N2 reactions, $F^- + CH_3Cl$ and $F^- + CH_3I$, and showed that depending on the kinetic energy of the nucleophile, the angle with which it approaches the substrate, and the leaving group, distinct reaction mechanisms are observed.[23] This was later rationalized by Hennig and Schmatz in terms of a quantum-mechanical study.[24] Very recently, Wester and co-workers quantified the atomic dynamics associated with S_N2 vs E2 reactions and analyzed product velocity distributions for reactive collisions, $X^- + RY$ (where X = Y = F, Cl, I and R = methyl, *iso*-propyl, and *tert*-butyl).[25] They established the dynamics of the reactivity preference shift, from substitution to elimination, as the degree of methylation increases. Dynamics calculations have revealed other mechanisms that are in competition with the Walden inversion, such as the 'roundabout'[26] and double inversion mechanism.[27] Similar to frontside attack, the double inversion mechanism is another possible route that results in retention of configuration. Xie and Hase recently reviewed the developments made towards elucidating novel reaction mechanisms.[28]

All of the aforementioned effects (e.g., solvent effect, competition with S_N1 or E2, reaction dynamics, or rotational effects in complex forming) would warrant a detailed overview on their own. Here, however, we focus on S_N2 reactions, as well as variations of the nucleophile and/or leaving group, variation of the central atom, bulkiness of the substituents, and how these might be exploited for the creation of pentavalent carbon. The quest for such a pentavalent species has challenged chemists for about a century[1a] and has recently been solved.[29]

2. Variation of Nucleophile and Leaving Group

2.1. Halide Nucleophiles and Leaving Groups

Halide ions (F^-, Cl^-, Br^-, I^-) are often used as nucleophiles and/or leaving groups in studies on S_N2 reactions.[4,30] Bento and Bickelhaupt have reported[30c] a systematic investigation on the nucleophilicity and leaving-group ability of the halides for the reaction $X^- + CH_3Y$ with X, Y = F, Cl, Br, I. Both the frontside and backside pathways (see Scheme 4) were explored using relativistic density functional theory at the ZORA-OLYP/TZ2P level. The Walden inversion associated with the backside attack leads to inversion of configuration. The stereochemistry of the resulting product may be scrambled, resulting in a racemic mixture if a second nucleophile (X^-) attacks the product (H_3C–X).

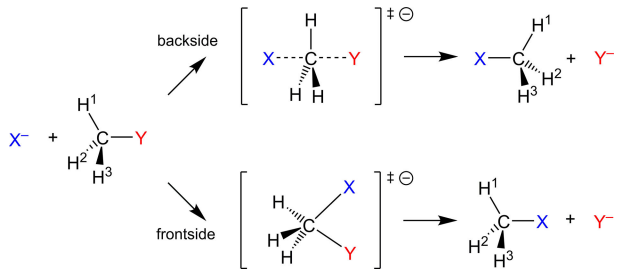

Scheme 4. General representation of the backside versus frontside pathway for $X^- + CH_3Y$ (X, Y = F, Cl, Br, I).

The reaction with X = Y = F was the only reaction where a double-well PES was observed for both the backside and frontside pathway. For all other combinations, there was at least one stationary point not present.[30c] For many of these cases, this results directly to the exothermicity of the reaction: it is not just the reaction energy that is affected, but also the intermediate points are pulled down (see Scheme 5). At a certain point, the exothermicity is so large that no barrier (and preceding reactant complex) exists any longer.

The frontside pathway is, in most cases, highly disfavored because of the increased steric repulsion as result of the proximity of the nucleophile and leaving group in the transition state. Focusing on the backside pathway, the reaction barrier was found to increase along the nucleophiles $F^- < Cl^- < Br^- < I^-$, and decrease along the substrates CH_3F, CH_3Cl, CH_3Br, CH_3I. Therefore, fluoride is the best nucleophile, and iodide the best leaving group. The combination of these two gives a reaction energy of -52.5 kcal mol^{-1} at ZORA-OLYP/TZ2P.[30c] These phenomenological trends had already been observed before, but the study by Bento and Bickelhaupt[30c] tried to address them in terms of a straightforward, causal relationship between the reactants' electronic structure and their S_N2 reactivity. They found that the nucleophilicity is determined by the electron-donor capability of the nucleophile (energy and shape of the X^- np atomic orbital), and the leaving-group ability is derived directly from carbon-leaving group (Y) bond strength.

The study of the origin of nucleophilicity was extended by Sauers,[31] after noting that the computed reaction barrier for halides with bis-ammonium alkyl dihalides showed an unexpected insensitivity to the nature of the halide. Instead, a very good correlation was found between the barrier height and the ionization potential of the nucleophile.[31] In contrast, no such clear correlation with the proton affinity (PA) was observed, a property which had been suggested previously by Uggerud[32] as an important factor related to nucleophilicity. Arnaut and Formosinho[33] used an intersecting/interacting-state model (ISM) to explain reaction barriers based on bond lengths, force constants, ionization potentials and electron affinities of the reactants. However, for the symmetrical (X = Y) S_N2 reactions of Scheme 4, it only worked well for X = Cl. For the other halides, deviations of 2–6 kcal mol^{-1} were found, while for X = Y = H an even larger discrepancy was observed.

Schleyer, Allen, and co-workers investigated[34] S_N2 identity reactions of methyl, ethyl, propyl, allyl, benzyl, propargyl, and acetonitrile halides (X = F$^-$, Cl$^-$) at the CCSD(T)/aug′-cc-pVTZ level with the goal of assessing the conventional view that π-conjugative effects facilitate S_N2 reactions. Their findings challenge the traditional view that acceleration of S_N2 reactions for systems with an adjacent multiple bond is the result of π-conjugation in the transition state. Instead, they propose a favorable substrate-nucleophile electrostatic interaction, which strongly dictates reaction rate trends. An attractive $X(\delta^-)\cdot C_\beta(\delta^+)$ interaction (lower net activation barrier) is found in the S_N2 TS for propargyl halides, whereas a repulsive $X(\delta^+)\cdot C_\beta(\delta^+)$ interaction (higher net activation barrier) exists for propyl halides. These electrostatic interactions were further explored and supported by other groups as well.[35]

2.2. Other Small Nucleophiles and Leaving Groups

There are a number of studies that focus on other nucleophiles and leaving groups.[36] In a series[4a–c] of papers, Schaefer and co-workers studied several combinations of nucleophiles and leaving groups; first[4a,b] for non-identity reactions with fluoride (F^-) as nucleophile, and several leaving groups (LG = F, Cl, CN, OH, SH, NH_2, PH_2). At the CCSD(T)/TZ2Pf + diff level it was shown that only Cl and SH are better leaving groups than F and lead to exothermic reactions. For the other leaving groups, the reactions are mildly (LG = CN) to substantially endothermic (LG = PH_2, OH, NH_2). Some time later they studied model identity S_N2 reactions with the same set of leaving groups and using the same group as the nucleophile (Nu = LG).[4c] The

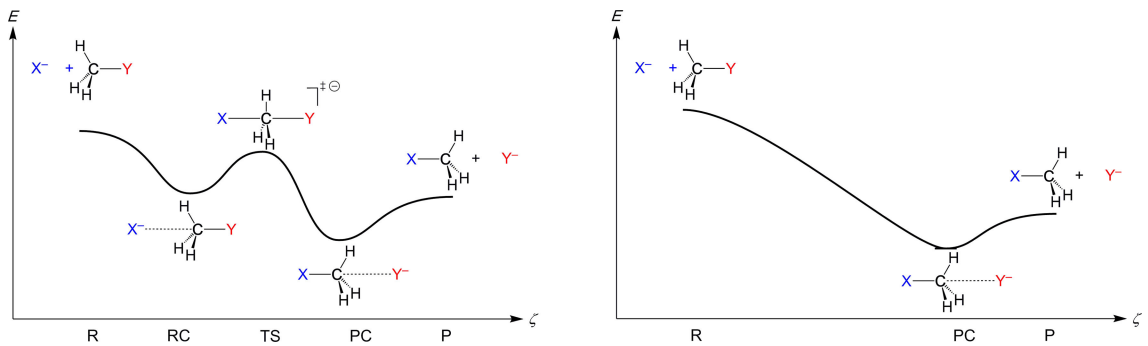

Scheme 5. Change of energy surface with increasing exothermicity of the reaction, resulting finally in a single-well (product-complex) PES.

overall barrier $\triangle E^{\ddagger,ovr}$ at CCSD(T)/TZ2Pf+diff was found to be low only for the halides (−0.4 kcal mol^{-1} for F, +2.6 kcal mol^{-1} for Cl), with overall barriers between 14 and 29 kcal mol^{-1} observed for the other groups. Note that these barriers are relative to reactants, not with respect to the reactant complex, which is formed first. The central barrier taken relative to the reaction complex shows higher values, ranging between 13 (F, Cl) and 46 kcal mol^{-1} (OH).[4c]

Uggerud[32] used almost the same set of nucleophiles-leaving groups, but included similar groups with elements from a period higher (LG = NH_2, OH, F, PH_2, SH, Cl, AsH_2, SeH, Br). Apart from the anionic reaction $X^- + CH_3X$, he also studied the cationic equivalent $XH + CH_3XH^+$. The barrier heights at the G2-level were found to decrease on going from left to right in the periodic table. For the anionic reaction (except the halides), the overall barrier was found to go down in energy as well when going down in the periodic table, e.g. with $\Delta H^{\ddagger,ovr}$ values of 28.2, 24.6 and 20.0 kcal mol^{-1} for NH_2^-, PH_2^- and AsH_2^- respectively. For the cationic reaction, going from the second period (e.g. NH_3, $\Delta H^{\ddagger,centr}$ 21.5 kcal mol^{-1}) to the third period (e.g. PH_3, $\Delta H^{\ddagger,centr}$ 32.3 kcal mol^{-1}) the barrier increases, but then decreases again upon going to the fourth period (AsH_3, $\Delta H^{\ddagger,centr}$ 28.4 kcal mol^{-1}). Ren and co-workers extended[37] the set of anionic nucleophiles with the carbon analogs CH_3^-, SiH_3^- and GeH_3^-, and used them for the reaction with ethyl chloride. They studied both elimination and substitution and found at the G2(+) level that the latter reaction was always favored under thermodynamic control; i.e. the S_N2 reaction energies were more favorable than the E2 ones. This was also found for reactions under kinetic control for the majority of the nucleophiles, except for F^-, OH^- and NH_2^- for which the elimination pathway was favored. For this CH_3CH_2Cl substrate, the hydroxide was found to be a better nucleophile than the fluoride.

Ren and Yamataka studied[38] the reaction between several other anionic nucleophiles (HO^-, HS^-, CH_3O^-, HOO^-, HSO^-, FO^-, ClO^-, BrO^-, NH_2O^-, $HC(=O)OO^-$) with CH_3FCl and CH_3F at the G2(+) level in the gas-phase. Their computations indicate that nucleophiles with an adjacent lone pair (α-nucleophiles) display enhanced nucleophilicity, a phenomenon known as the α-effect.[39] By plotting the overall barrier for substitution vs the proton affinity (PA) of normal nucleophiles (i.e. nucleophiles lacking an adjacent lone pair), a good correlation was revealed, thus indicating that the relative reactivity is controlled by the PA of the nucleophile, in line with activation strain analyses by Bento and Bickelhaupt.[30c] Interestingly, a downward deviation from this barrier vs. PA correlation was found for all α-nucleophiles. The origin of the enhanced reactivity of α-nucleophiles is attributed, amongst others, to a reduction of the deformation energy associated with reaching the TS. In a later study, Bierbaum and co-workers[40] measured reaction rate constants and deuterium kinetic isotope effects for the reactions of BrO^- and ClO^- with RCl (R = Me, Et, *iso*-propyl, *tert*-butyl). They found that these α-nucleophiles, along with the HOO^- nucleophile, did not display enhanced reactivity compared to normal nucleophiles. These findings were interpreted as the α-effect not being an intrinsic property of the anion in the gas-phase, but rather arising due to a solvent effect. A few years later, however, the same laboratory arrived at the opposite conclusion and obtained experimental validation of the α-effect in the gas-phase from a thorough thermochemical analysis.[41] The influence of solvation was then reinvestigated Bierbaum and co-workers,[17c] through the investigation of the gas-phase reactivity of monosolvated nucleophiles. It was found that coordination of a single water molecule to the nucleophile resulted in a smaller PA and higher barrier compared to unsolvated nucleophiles. Interestingly, however, reaction efficiency decreases faster as a function of PA for monosolvated nucleophiles compared to their unsolvated counterparts. Furthermore, weaker hydrogen bonding interactions between the explicit water molecule and the α-nucleophile, compared to a normal nucleophile, may result in differential solvation and could be another contributing factor to the α-effect. Despite these developments, the existence of whether or not the α-effect exists is still a matter of debate.[42]

2.3. Counter-ion-Assisted S_N2 Reactions

A number of studies have been performed where the nucleophile or substrate is accompanied by a counter-ion such as Li^+, Na^+ or K^+.[43] The clearest example of counter-ion effects on the nucleophile was shown by the study of Ebrahimi and co-workers,[43c] who studied the nucleophiles X^-, Li^+X^-, Na^+X^-, K^+X^- with the substrates CH_3X (X = F, Cl, Br). The reactions were clearly disfavored by the counter-ion, e.g. the central barrier for X = F at QCISD (T)/6-311++G(d,p)//MP2/6-311++G(d,p) increased from 13.7 kcal mol^{-1} for Nu = X^-, to between 48.0 and 67.4 kcal mol^{-1} for Nu = Li^+X^-, Na^+X^-, K^+X^-. Interestingly, the frontside pathway was favored by the presence of the counter-ion, most noticeably the case of Li^+F^-, which had a barrier that was some 10 kcal mol^{-1} lower than that of the corresponding backside pathway. Nevertheless, it is still disfavored by ca. 36 kcal mol^{-1} with respect to the pathway without the counter-ion (see Figure 1).

de Cózar and co-workers investigated[43g] ion-pair S_N2 reactions of model systems ($M_nF^{n-1} + CH_3Cl$ ($M^+ = Li^+$, Na^+, K^+, and $MgCl^+$; n = 0, 1) at OLYP/6-311++G(d,p) by means of the activation strain model.[8] The introduction of a counter-ion

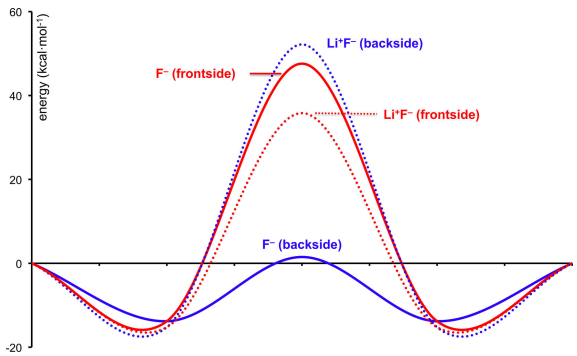

Figure 1. Effect of counter-ions on energy profile (based on data from ref.[47c])

raises S_N2 barriers because the counter-ion stabilizes the nucleophile's HOMO, i.e., it makes the nucleophile a weaker Lewis base. This, in turn, results in a much weaker interaction between the nucleophile and the substrate. The preference for the frontside pathway is enhanced in the case of the second-row counter-ions. Molecular orbital analysis revealed that these ions are more compact and have a lower-energy LUMO, which enables a more stabilizing interaction with the leaving group in the cyclic frontside attack TS. This feature was most prominent in the case of $M^+ = MgCl^+$, where the frontside pathway is preferred in the gas-phase as well as in solution.

Marié, Courillon, and Malacria[43a] reported how the counter-ion could be beneficial as well, in S_N2' reactions between lithiated carbon nucleophiles and silylated vinyloxiranes. Diastereomeric ratios of over 7 to 1 in favor of Z olefins were observed. This followed earlier work by Bickelhaupt and co-workers who studied nucleophilic cleavage with organolithium reagents.[2f]

2.4. Bulky Nucleophiles and Leaving Groups

In addition to the smaller nucleophiles described above, larger ones have been systematically studied as well.[44] Bickelhaupt and co-workers studied the reaction of halomethyl anions XCH_2^- (X = Cl, Br) with CH_3X and NH_3, to form XCH_2CH_3 and CH_3NH_2, respectively.[2e] This was followed by a later study of the reaction between other anionic bases (NH_2^-, $C_6H_5^-$, OH^-, $CH_2{=}CH{-}CH_2^-$) and tetrahydrofuran. Both studies assessed the reactivities of the nucleophiles and the preferences for either nucleophilic substitution or elimination.

Savelli and co-workers[45] studied the role of reverse micelles in S_N2 displacements by bromide ions. The reagents were quite diverse (anionic, neutral, cationic), involving methylnaphthalene-2-sulfonates (see Scheme 6), with substitutions on the

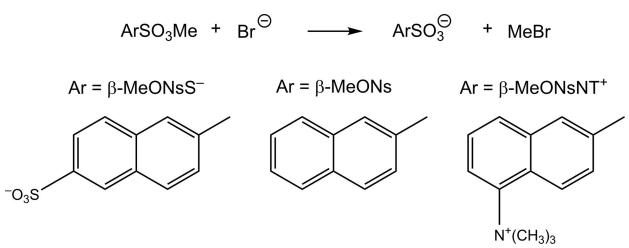

Scheme 6. Methylnaphthalene-2-sulfonates used by Savelli et al.[22]

naphthalene moiety giving the change in molecular charge. The rate constants increased significantly from the neutral ($8.0 \cdot 10^5\ M^{-1}\,s^{-1}$) to the anionic ($10.0 \cdot 10^5\ M^{-1}\,s^{-1}$) to the cationic form ($41.5 \cdot 10^5\ M^{-1}\,s^{-1}$).[45] Moreover, the reactions were accelerated by aqueous micelles of cetyltrimethylammonium bromide (CTABr). Westaway and co-workers also used an alkylbromide substrate, but instead of varying the nucleophile, they used different leaving groups.[46] They studied the kinetic isotope effects (KIEs) and nucleophile $^{11}C/^{14}C$ isotope effects for the reaction between tetrabutylammonium cyanide and ethyl iodide, bromide, chloride, and tosylate. The fastest reaction was with iodide as leaving group ($10^{-1}\ M^{-1}\,s^{-1}$), followed by bromide ($10^{-2}\ M^{-1}\,s^{-1}$), tosylate ($10^{-3}\ M^{-1}\,s^{-1}$) and chloride ($10^{-4}\ M^{-1}\,s^{-1}$). The bulky tosylate is thus an order of magnitude faster than the much smaller chloride.

Ji, Atherton, and Paige reported[47] the S_N2 reaction of benzyl chloride with nucleophiles in liquid ammonia. Interestingly, two opposing trends were observed: for the anionic nucleophiles, the reaction rate decreases with *decreasing* size of the nucleophile. For neutral nucleophiles, the reaction decreases with *increasing* size. Both are probably resulting from the effect of the solvent, which stabilizes the smaller anionic reagents more than the larger ones. Therefore, the effect of the bulkiness of the nucleophiles is difficult to extract from these data.

Bach and co-workers investigated the mechanism of disulfide bond cleavage by using sulfur[48] and phosphorus[49] nucleophiles. The sulfur nucleophiles ranged from methyl- and ethylsulfide to the bulky *tert*-butyllsulfide, and followed earlier studies by Bachrach and co-workers on simpler nucleophiles.[50] Since not only the nucleophile but also the substituents of the central atoms were substituted at the same time, it is difficult to separate the effect of the nucleophile size from that of the substituents (see also the S_N2@S section below). The study with the trimethylphosphine[49] nucleophile showed the reaction to be highly endothermic.

Mahmood et. al. studied the ambident reactivity of substituted nitronates (*C*- or *O*-alkylation) in the S_N2 reaction with CH_3I using *ab initio* MP2/CBS method, RRKM theory, and kinetic simulations.[51] Contrary to previously proposed reaction mechanisms involving a preference for *O*-alkylation, they show that *C*-methylation is the preferred, both thermodynamically and kinetically.

Ren and co-workers[52] developed a convenient method that is both mild and regioselective, for the *N*-alkylation of 2-pyridones in water. 2-Pyridones are ambident nucleophiles, which can undergo either *N*- or *O*-alkylation, and serve as important precursors for complex natural products and pharmaceuticals.[53] These "green" reaction conditions employed Tween 20 to assemble a micellar system that enhanced the nucleophilicity of the 2-pyridone to afford a significant preference for *N*-alkylated adducts.

3. Variation of Central Atom

The prototypical S_N2 reactions take place with carbon as the central atom, and often using halides as nucleophiles and/or leaving groups.[4f] This normally leads to the double-well PES shown in Scheme 2. The nature of the central atom is unequivocally important for the shape of the PES as we will discuss in this section. An important issue is the character of the central species, which is typically an energy maximum for first-row elements (transition state involving a barrier, see Scheme 7, left), and a minimum for second-row elements (transition complex, Scheme 7 right).

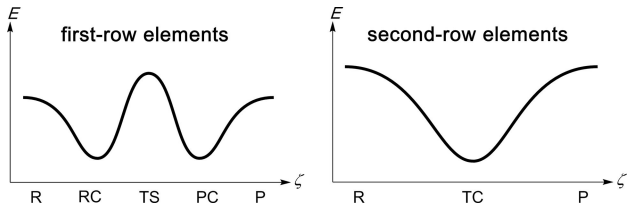

Scheme 7. Typical energy surfaces for S_N2 reactions at first-row elements (left) and second-row elements (right).

3.1. S_N2@Si

Holmes has reviewed the stereochemistry of nucleophilic substitution at tetracoordinated silicon,[54] which was followed by reviews by Corriu and co-workers[55] on the reactivity of penta- and hexacoordinate silicon compounds, and a review on the chemistry and thermochemistry of silicon-containing anions in the gas-phase by Damrauer and Hankin.[56] A recurring theme in all of these reviews is the existence of stable, hypervalent (penta- or hexavalent) silicon compounds.

In 2005, Bento et. al. performed an *ab initio* and DFT benchmark study for nucleophilic substitution at carbon (S_N2@C) and silicon (S_N2@Si).[57] The study focused on the reaction with Cl^- as nucleophile and leaving group, using both density functionals (BP86, BLYP, OLYP), Hartree-Fock (HF), and post-HF methods such as Møller-Plesset second- and fourth-order perturbation theory (MP2, MP4SDQ) and coupled cluster CCSD(T). The effects of relativistic scalar corrections were also accounted for through the use of the zeroth-order regular approximation[58] (ZORA-OLYP). The study displayed the expected energy profiles (see Scheme 7) for the reaction at carbon and silicon, with a transition state (TS) for carbon and a stable transition complex (TC) for silicon. The TC complex for silicon was ca. -27 kcal mol^{-1} compared to reactants at CCSD(T)/aug-cc-pVQZ. The TS of carbon was instead found at 2.5 kcal mol^{-1} compared to reactants and involved a central barrier of ca. 12.9 kcal mol^{-1}.[57] Both the shape and well depths were adequately represented by the OLYP density functional, which resulted in differences of only 2–3 kcal mol^{-1} compared to the CCSD(T) calculations. The effect of the relativistic corrections was, as to be expected, negligible (<0.1 kcal mol^{-1}); these corrections usually start to play a role from the fourth period upwards (see e.g. refs. [59] and [60]).

Following upon a prior study on the disappearance and reappearance of reaction barriers in reactions on phosphorus,[61] Bento and Bickelhaupt published in 2007 a remarkable study[62] on substitution reactions at silicon that proceed via a central reaction barrier. The objective of that study[62] was to understand *why* the central barrier disappears from S_N2@C to S_N2@Si (and also Ge, Sn and Pb[63]) despite the fact that these processes are isoelectronic and isostructural. Various reactions were explored with different substituents on the central atom, i.e. CR_3Cl and SiR_3Cl with R = H, CH_3, C_2H_5, and OCH_3. Their results showed that the nature of the S_N2 reaction barrier is, in essence, steric based, but could also be modulated by electronic factors. Hence, by simply increasing the steric demand of the substituents R around silicon (see Figure 2), the S_N2@Si mechanism changes from its regular single-well PES (R = H), via a triple-well PES (R = CH_3, R = C_2H_5, with a pre- and post-TS before and after the central TC) to a double-well PES (R = OCH_3), which is normally encountered for S_N2@C reactions. The energy surfaces were subsequently further analyzed with the activation strain analysis.[8] This analysis showed that the central barrier disappears when going from S_N2@C to S_N2@Si for two reasons. First, the steric congestion at the larger silicon atom is reduced and second, because the nucleophile-substrate interaction is more favorable in the silicon case. This suggests that simply by sufficiently increasing the steric bulk of the substituents R, the mechanism for S_N2@Si would be changed into a double-well PES with a central barrier. Their study[62] with different substituents showed that at least methoxy groups are needed to achieve this. The driving force for this steric congestion was found to be Pauli repulsion that is gradually being converted into substrate strain.

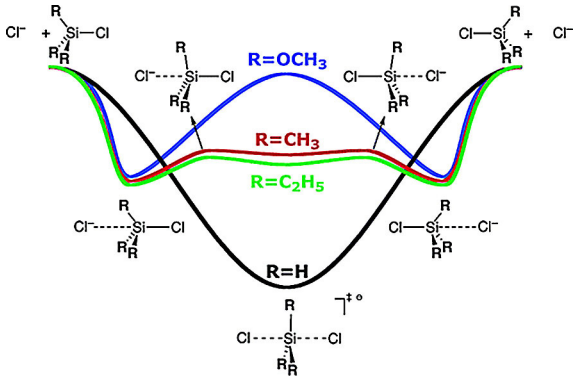

Figure 2. Change of potential energy surface (PES) for S_N2@Si with different substituents R (H, CH_3, C_2H_5, OCH_3) around silicon (from ref.[62]).

In a follow-up paper,[9b] van Bochove et al. reported the effect of solvent on the S_N2@C and S_N2@Si reactions. They showed that solvation causes in both cases a unimodal reaction profile with a single barrier to product formation.

3.2. S_N2@P

Recently, Kolodiazhnyi reviewed the stereochemistry of nucleophilic reactions at phosphorus[64] Holmes reviewed the similarities and differences between silicon and phosphorus,[65] and Cavell and co-workers reviewed neutral six-coordinate phosphorus.[66] However, in the current review, we wish to feature the fact that nucleophilic substitution at phosphorus proceeds mainly through a stable transition complex, similar to silicon.

In 2006, van Bochove et al. reported[61] for the first time the mechanism for an S_N2 reaction at phosphorus that proceeds through a central barrier. Their investigation involved a systematic study on the influence of substituents on the energy profile, where both the number of substituents, as well as their electronic properties and size were modulated. Apart from the S_N2@C and S_N2@Si reactions that were included for comparison,

they studied either tricoordinate phosphorus PR_2Y (S_N2@P3) or tetracoordinate phosphorus $P(=O)R_2Y$ as substrate (S_N2@P4):

$$X^- + PR_2Y \rightarrow PR_2X + Y^- \qquad (\mathbf{1}: SN2@P3)$$

$$X^- + (P{=}O)\ R_2Y \rightarrow (P{=}O)\ R_2X + Y^- \qquad (\mathbf{2}: SN2@P4)$$

The size and nature of the phosphorus substituents R were quite diverse, from hydrogen to the small and electronegative F, bulky polarizable Cl, methyl groups, and finally methoxy groups. The nucleophile and leaving group in the symmetric (X=Y) reactions **1** and **2** were taken as either Cl^- or OH^-. With single-atom substituents R (H, F, Cl), the energy surface remained a single-well PES with a stable central complex TC (see Scheme 7). The depth of the well was, for the X=Y=Cl series, smaller (i.e. less stable) for the more crowded tetracoordinate phosphorus than for the tricoordinate isomer. Moreover, the well depth decreased along the ligand series H>F>Cl (with values of respectively −26.2, −24.7, and −23.3 kcal mol^{-1} at OLYP/TZ2P for reaction **1**), revealing that bulkier substituents result in less stable central transition complexes. In contrast, with the hydroxide nucleophile (X=Y=OH), the tetracoordinate phosphorus was more stable because of hydrogen bonding between the phosphoryl unit P=O and the incoming and outgoing OH groups.

The first change in the energy profiles for these reactions at phosphorus was observed with S_N2@P4 and R=Cl (see red curve in Figure 3). The PES transformed into a triple-well PES,

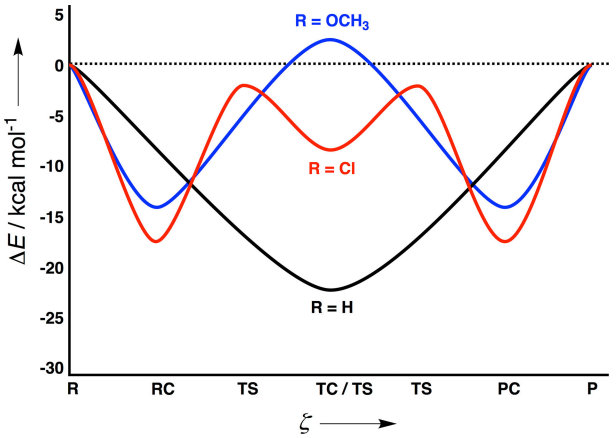

Figure 3. Reappearance of reaction barriers for S_N2@P (from ref.[61]).

where the central species was still a stable TC, at −8.4 kcal mol^{-1} compared to the reactants. However, the reaction also involved a reactant and product complex (at −17.5 kcal mol^{-1} compared to the reactants), which were separated from the TC by a pre-TS and post-TS. The barrier between the RC and TC was still substantial (ca. 15 kcal mol^{-1} at OLYP/TZ2P). Further increasing the steric bulk (with $R=OCH_3$ and S_N2@P4) led to a merging of the pre-TS and post-TS barriers, thus resulting in a double-well potential (see blue curve in Figure 3) where the central species is a transition state (as is usually observed for S_N2@C). The reactant complex is more or less the same as with R=Cl (at −14.1 kcal mol^{-1} compared to reactants), and it is really the central species that is destabilized (at 2.5 kcal mol^{-1} compared to reactants, i.e. involving a central barrier of ca. 17 kcal mol^{-1} at OLYP/TZ2P). These trends were not affected by the level of theory, i.e. either increasing the basis set to QZ4P, or changing the density functional to mPBE0KCIS (the best performing one for S_N2 reaction barriers[9f]) did change the energies by a few kcal mol^{-1}, but not the shape of the energy profiles. Also, the electronic properties of the nucleophile and leaving group are important, because the double-well PES for the energy surface was observed mainly for the chloride nucleophile, and not for hydroxide. In the latter case, a triple well is observed with pre- and post-TS, and the TC species is more favored than the RC because of hydrogen-bonding between the P=O unit and the hydroxyl groups.

This study on S_N2@P was later[67] extended to include also asymmetric (X≠Y) frontside and backside reactions and determination of the influence of reactant conformation on the reaction mechanism. The single-well PESs were also observed for the asymmetric reactions, and in general small differences were found between S_N2@P3 and S_N2@P4. However, the latter exhibits a characteristic that it shares with S_N2@Si, but not with S_N2@P3: introducing sufficient steric bulk around the central atom causes the appearance of pre- and post-barriers that separate the TC from the reactant and product complexes. Surprisingly, these extra features appeared to be present also when the overall reaction becomes significantly exothermic (e.g. −71 kcal mol^{-1} at OLYP/TZ2P for $OH^- + (P{=}O)Cl_3$). A second interesting feature was observed for reactions involving the OH^- nucleophile, where different reaction channels occur (with sometimes different products formed). Finally, the backside pathway sometimes competes with frontside pathways where instead of the anticipated leaving group Y, one of the substituents R is expelled.

Another paper by van Bochove[68] extended upon the systems even further by including CH_3O^- as nucleophile, leaving group, and ligand. This leads (again) to a dramatic change in the energy profile for the reaction. In general, the nucleophilic substitution is accompanied by the Walden-inversion[1a] that proceeds as the concerted umbrella motion of the substituents at the central atom, and either via a labile TS or stable transition complex. However, with the larger substituents around the phosphorus, it was observed that Walden-inversion can also proceed step-wise, in which the individual substituents flip consecutively, from the educt to the product conformation.

These individual "Walden-flipping" events occur through clockwise or counterclockwise rotation of the OMe substituents at the central phosphorus atom around their P–O bond and involve separate barriers on the reaction profile (see Scheme 8).

In a very recent study[69] by van Bochove, the hydrolysis of phosphate esters was studied to gain insight into one of the most fundamental biochemical reactions. Hydrolysis of triphosphate (PPP) occurs during the replication of DNA in all living systems and proceeds via a key S_N2@P step.[70] DNA synthesis is catalyzed by Mg^{2+}, which speeds us this otherwise remarkably

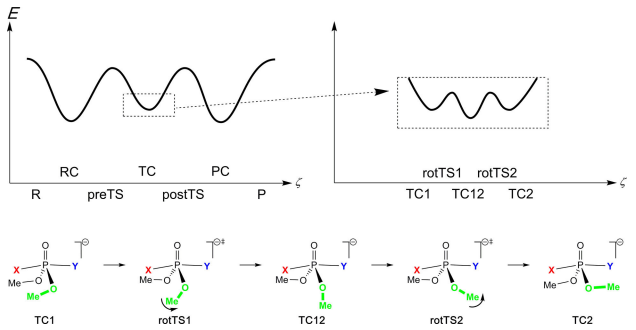

Scheme 8. Stepwise Walden-flipping and associated structures showing rotation of the MeO substituent.[68]

slow biological reaction.[71] An activation strain analysis revealed that the origin of the Mg^{2+} counterion's catalytic nature manifested from two mechanisms: 1) weakening of the P^{α}–O^{α} leaving group bond (decreased activation strain) and 2) transition state stabilization by decreasing the net negative charge of the fully deprotonated PPP, in addition to stabilization of the LUMO of PPP (increased interaction). These effects, in tandem, sufficiently lower the barrier for enzymatic PPP hydrolysis and yields biologically feasible activation barriers.

The inertness of P–C bonds were recently studied by Ashkenazi and co-workers[72] at the PCM–B3LYP/6-31+G(d) level when they investigated chloro-substituted methylphosphonated esters. In these systems, an attacking hydroxide can either lead to P–C cleavage (**3**) or ester hydrolysis (**4**):

$$OH^- + Cl_{3-n}H_nC(P{=}O)(OMe)_2 \rightarrow HO\text{-}(P{=}O)(OMe)_2 + CH_nCl_{3-n}{}^- \quad (3)$$

$$Cl_{3-n}H_nC(P{=}O)(OMe)(OH) + OMe^- \quad (4)$$

Interestingly, the energetic preference for either pathway depends on the number of chloride substituents at the methyl group: the nonsubstituted reactant undergoes exclusively P–O bond cleavage (**4**), while the trichlorinated analog proceeds exclusively through P–C bond dissociation (**3**). Monitoring any possible toxic degradation products is of interest to the agrochemistry field and involves assessing the stability of these P–C bonds.[72] Detoxification of extremely toxic chemical warfare agents such as VX, GB (sarin) and sulfur mustard is an active field of research, wherein Ganguly and co-workers recently reported[73] the solvolysis of *P*-[2-(dimethylamoino) ethyl]-*N*,*N*-dimethylphosphonamidic fluoride (GV), an example of a series of nerve agents. They studied the attack of three nucleophiles (hydroxide HO^-, hydroperoxide HOO^-, and hydroxylamine anion NH_2O^-) on GV, which has a fluorine substituent on phosphorus that acts as leaving group. Reaction with the hydroperoxide nucleophile was kinetically favored, as it benefited from strong intermolecular hydrogen bonding in the TS geometry. The assistance of a water molecule affects the activation barrier, and indeed solvation is needed for the destruction of GV.

3.3. S_N2@S

A number of studies have focused on S_N2 reactions at sulfur, involving numerous combinations of nucleophiles and leaving groups.[74] Bachrach and Mulhearn reported the first *ab initio* study in 1996[50a] on the reaction mechanism of nucleophilic substitution at sulfur and identified a competition between S_N2 and addition-elimination pathways. Different combinations of the substituents R at sulfur were studied for the reaction $R_1S^- + R_2SSR_3 \rightarrow R_1SSR_2 + R_3S^-$, and depending on the level of theory used, either the S_N2 or addition-elimination was favored. Inclusion of electron correlation in CCSD(T)/6-31+G(d) showed the reaction follows a triple-well PES in the gas-phase. This was later confirmed by Ramos, Bickelhaupt, and co-workers[75] who used the OPBE and BP86 density functionals in conjunction with large basis sets (TZ2P). The latter study also showed that the energy profile changed again when including solvent effects. Houk and co-workers[76] studied the radical substitution reactions involving $CH_3^{\bullet}$ as the nucleophile and determined they proceed via an S_N2 pathway with central transition states.

Reactions at S–S bonds are particularly interesting due to their presence in biological systems in the form of cystine bridges in proteins. These bridges are often involved in or affected by, redox processes, in which a disulfide bond may interconvert with a dithiol system.[77] Bachrach and co-workers[50,78] highlighted other reaction mechanisms to achieve S–S bond cleavage. Their work was expanded on by Ramos, Bickelhaupt, and co-workers.[75,79] Orian and coworkers further investigated reactions involving other chalcogens by focusing on S_N2@S, S_N2@Se, and S_N2@Te.[74j] Bachrach and co-workers studied simple acyclic also investigated cyclic sulfides[50b,74a] and sulfinyl derivatives.[78] In the latter compounds, the additional oxygen ligand to sulfur does not have a marked effect on the energy surface and the reaction proceeds mainly through a triple-well mechanism. The only exception found was with cyanide as the nucleophile, which showed a double-well PES, albeit with a very small barrier.[78] The study by Bachrach and Chamberlin on cyclic sulfides[50b] was the first step towards understanding the S_N2@S processes in biological systems. Their bicyclic geometry was the smallest peptide that contains a disulfide bridge, which could exist in a configuration with a positive dihedral angle (***P***), or with a negative (***M***) one (see Scheme 9). The attack by HS^- displayed a triple-well energy surface.

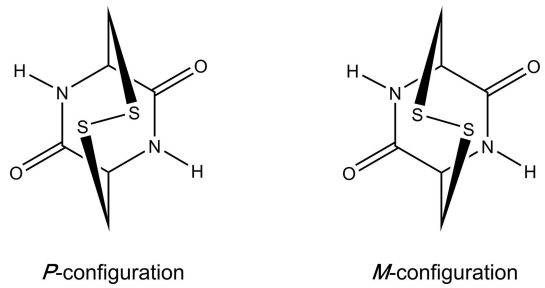

Scheme 9. Bicyclic peptides studied by Bachrach and Chamberlin.[50b]

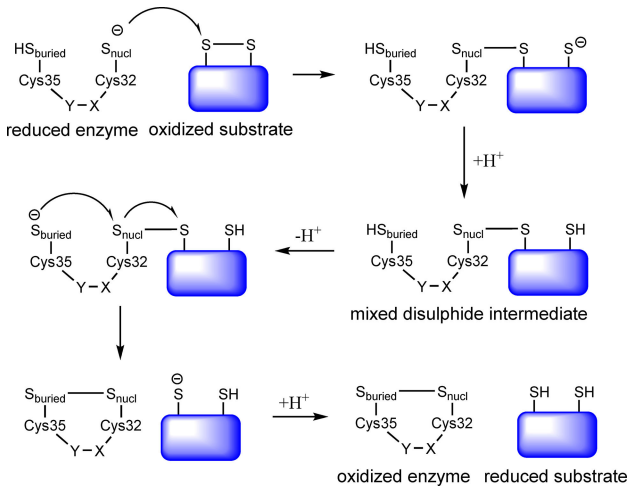

Scheme 10. Mechanism of Trx-catalyzed reduction of disulfide bonds.

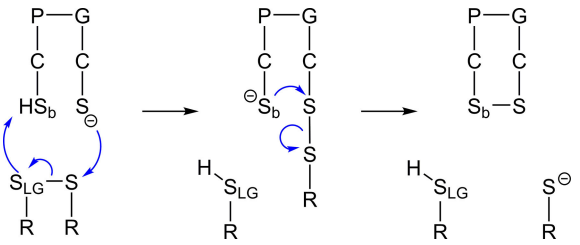

Scheme 11. Involvement of the leaving group S_{LG} in the deprotonation of buried thiol S_b.

Ramos, Bickelhaupt, and co-workers[75,79] extended the studies to biologically relevant disulfides significantly using both quantum-chemistry (QM) and molecular-dynamics (MD) techniques. The QM study was performed on a system that contained all amino acid residues present in the active site of thioredoxin (Trx), with a characteristic CXYC motif, together with dimethyl disulfide as a model for the substrate (see Scheme 10).

These QM studies were complemented by classical MD simulations[75] on the model active sites and the complete enzyme-substrate complex, with and without explicit solvent molecules. Two different enzyme motifs were studied in order to probe how the activity of the thioredoxin enzyme might be determined by the structural rigidity of the variable residues XY. This was performed for both the model systems, i.e. CGPC and CGGC, and the enzyme, i.e. wildtype Trx and its P34G mutant.

An important caveat about the above mechanism is that deprotonation of the thiols activates them for the $S_N2@S$ substitution. This is, in particular, true for the buried thiol Cys35, for which it was hypothesized that Asp26 could be responsible. The problem with this hypothesis was the distance between Asp26 and Cys35 (6 Å), which might, however, decrease while the reaction takes place. Nevertheless, the MD simulations on wildtype Trx[75] showed almost no variation for this distance and therefore an active role of Asp26 was ruled out.

The solution to this problem came from the QM study on the model systems and indicated an additional role of the leaving group from the first $S_N2@S$ step, which was not observed previously. This leaving group reorients itself and deprotonates the buried thiol, thereby activating it for the second $S_N2@S$ step (see Scheme 11).

In a follow-up study,[79] the authors also examined other CXYC motifs that are observed in other members of the protein family. For instance, apart from Thioredoxin (XY = GP), there are also the Glutaredoxin (XY = PY), protein disulfide isomerase (XY = GH) or disulfide bond formation A (XY = PH) proteins.

Finally, let us mention a recent experimental study[80] on force-activated $S_N2@S$ reactions. The authors found that hydroxide anion mediated cleavage of a protein disulfide bond proceeds with an abrupt reactivity switch at a force of ca. 500 pN. Several scenarios were discussed by the authors, based on the PES having either a double-well surface, or a triple-well surface, or involving a conformational change induced by the applied force. Using *ab initio* molecular dynamics simulations to study a model diethyl disulfide system in water, Dopieralksi et. al. rationalized[81] the experimentally observed reactivity switch (at 500 pN) that was observed in the original experimental study. They found that the external force accelerates the bond cleavage by performing work along the mechanical coordinate. However, at forces > 500 pN an unfavorable distortion of the S–S–C–C dihedral angle of the disulfide moiety is observed, thus resulting in a conformer that is less prone to nucleophilic attack due to steric hindrance effects that prevented the hydroxide from an optimal attack of the two sulfur sites.

4. Bulkiness of Substituents

Bulky substituents play a significant role in the mechanism as highlighted by the studies by Bickelhaupt and co-workers on the $S_N2@P$[61] and $S_N2@Si$[62] reactions, which showed the disappearance of reaction barriers for small substituents (R = H) and reappearance of barriers for larger substituents ($R = OCH_3$) (see Figures 2 and 3). This can be rationalized in terms of steric interactions between the substituents, i.e. as they become larger and larger the steric crowding around the central atom increases, and hence a larger effort is needed to cross the barrier. This is for instance also shown in a study by Ren and Yamataka,[42d] who studied the reaction of $Nu^- + RCl$ with a variety of substrates. The reaction barrier $\Delta H^{\ddagger,ovr}$ at the G2(+) level was found to increase from 2.4 kcal mol^{-1} for R = methyl, to 4.5 kcal mol^{-1} for R = ethyl and 6.1 kcal mol^{-1} for R = *iso*-propyl. Recently, Bierbaum, Westaway, and co-workers studied[9a] the reaction of cyanide with alkyl iodides experimentally and found a decrease in rate constant with increasing alkyl size. Specifically, for CH_3I, the rate constant was 12.8 ± 0.3 (10^{-11} cm^3 s^{-1}), which dropped to 2.99 ± 0.02 (10^{-11} cm^3 s^{-1}) for CH_3CH_2I, and to less than 0.1 (10^{-11} cm^3 s^{-1}) for $(CH_3)_3CI$.[9a] Brauman and co-workers[82] studied steric effects in ionic S_N2 reactions for $Cl^- + RCH(CN)Cl$ and found similarly a decrease in the reaction rate for R = Me ($10.0 \cdot 10^{-12}$ cm^3 s^{-1}), R = Et ($8.9 \cdot 10^{-12}$ cm^3 s^{-1}), R = *iso*-propyl ($2.7 \cdot 10^{-12}$ cm^3 s^{-1}) and R = *tert*-butyl ($1.1 \cdot 10^{-12}$ cm^3 s^{-1}). The steric effect of a larger ligand was further confirmed in a computational study by Houk and co-workers that showed that the steric effect

of a *tert*-butyl group raises the activation energy by 6.3 kcal mol^{-1} relative to methyl.[83]

Gilheany and co-workers employed a combined nuclear magnetic resonance (NMR) and computational study to investigate reaction rates and energy barriers of degenerate halide substitution on tetracoordinate halophosphonium cations.[84] Both techniques point to a two-step mechanism associated with the formation of the pentacoordinate dihalophosphorane TC. The reaction first involves backside attack, then followed by dissociation, ultimately involving inversion of configuration at the central phosphorus atom. In addition, they studied the effect of substituents, (Me, Et, *iso*-propyl, *tert*-butyl) and determined that as the bulk increased, the reaction rate decreased. Bulky substituents had a destabilizing effect on the central TC, thereby raising the barrier and eventually resulting in a labile TS. In a follow-up study, Gilheany and co-workers again turned to NMR techniques and this time measured the dynamic exchange of two different halogens at a tetrahedral phosphorus center.[85] The free-energy barrier of activation was calculated to be around 11 kcal mol^{-1} for the triphenyl halophosphonium salt and was found to increase rapidly as the steric bulk increased from Me, Et, *iso*-propyl, *tert*-butyl, to other sterically bulky groups. This work shows that nucleophilic attack at the tetrahedral phosphorus center results in inversion of configuration.

Interestingly, the presence of bulky substituents is however not always unfavorable, as for instance shown by the "benzylic effect". A marked increase of S_N2 reaction rates is observed for benzylic systems compared to analogous alkyl derivatives (see ref. 86 and references therein). Allen, Schaeffer, and co-workers studied identity exchange reaction of $F^- + C_6H_5CH_2F$ and the analogous chloride reactions, using both a focal-point methodology (involving coupled cluster CCSD(T)) and the B3LYP density functional. Indeed, these computations showed the "benzylic effect" and quantified it as 3.8 kcal mol^{-1} for the fluoride reaction, and 1.6 kcal mol^{-1} for the chloride reaction. The origin of the effect was found to be related to the electrostatic potential V_C at the carbon reaction center, as confirmed also by the activation strain analysis for the reaction. It was also found that the benzylic effect could not be recovered by simply analyzing the NBO atomic changes, but required the mapping of the potential on the isosurface of the electron density.

Another study that showed rate acceleration with increasing ligand size was for nucleophilic substitutions at aziridine[87] (see Scheme 12). Banks used MP2 calculations to show that the

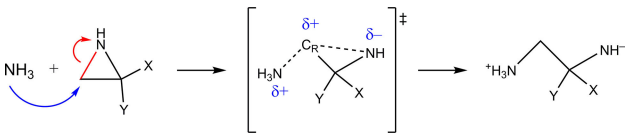

Scheme 12. Reaction of ammonia with haloaziridines.

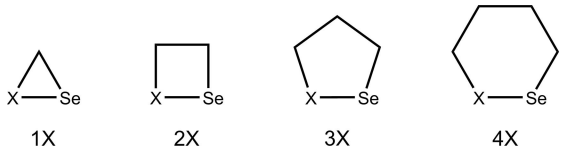

Scheme 13. Diselenide and selenyl sulfide substrates (X = Se, S).[54]

activation barrier $\Delta H^{\ddagger}$ decreased from 63.4 kcal mol^{-1} for X = Y = H to 33.0 kcal mol^{-1} for X = Y = Cl, and to 31.5 kcal mol^{-1} for X = Y = Br.

Bachrach and co-workers[88] also studied the effect of strain on reactivity, but then for a series of cyclic diselenides and cyclic selenyl sulfides (see Scheme 13). Smaller cyclic systems (e.g. **1X**), with larger strain, were found to proceed via ring opening reactions with lower barriers $\triangle E^{\ddagger,ovr}$ with B3LYP and MP2. For example, the TS for the reaction with HS^- is found at −15.1 kcal mol^{-1} with respect to reactants for **1Se** and becomes less favorable as ring strain is relieved, −14.3 kcal mol^{-1} (**2Se**), −14.2 kcal mol^{-1} (**3Se**), −13.7 kcal mol^{-1} (**4Se**, *chair*) and −9.0 kcal mol^{-1} (**4Se**, *boat*) at B3LYP/6-31 + G(d).

Liu and co-workers studied[55] the reaction of fluoride with $CR_1R_2R_3F$, and used quite a number of groups for R_1, R_2 and/or R_3. They used the B3LYP density functional to investigate how the larger groups might slow the reaction because they effectively block the backside approach of the incoming nucleophile. The central barriers $\Delta E^{\ddagger,centr}$ range in values from 1.5 kcal mol^{-1} for $R_1 = R_2 = R_3 = p$-Ph(NO$_2$)HH to 74.8 kcal mol^{-1} for $R_1 = R_2 = R_3$ = OHFF. The former value of 1.5 kcal mol^{-1} is probably underestimated, as it is well documented[4f,86] that B3LYP has a propensity to do so, but it is getting close to the objective of several studies discussed in this mini-review, i.e. the creation of pentavalent carbon (see below). Moreover, the authors[89] decomposed the barriers into different components such as steric contributions and quantum effects. In accordance with experimental findings, they found that the steric effects dominated the TS barrier.

Gronert and co-workers used salts of dianions (see Scheme 14) in order to be able to distinguish with mass spectroscopy the reaction products of the competing S_N2 and E2 pathways.[90] The E2/S_N2 ratio was found to largely depend on the size of the substrate:[90a] for ethylbromide it was less than 0.01 (i.e. almost exclusively S_N2 products), while for *tert*-butyl bromide the ratio was >200 (i.e. almost only E2 products).

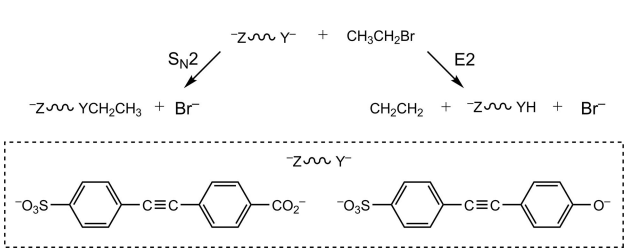

Scheme 14. Gas-phase reactions of dianions with alkyl bromides.[56a]

5. Creation of Pentavalent Carbon

The propensity to localize or delocalize bonds is an important issue for the design of truly pentavalent carbon compounds. Lithium and silicon have the capability to form hypervalent structures, such as Li_3^- and SiH_5^-, unlike their isoelectronic counterparts H_3^- and CH_5^-.[91] These latter compounds have a distortive, bond-localizing propensity. The discriminating factor between, carbon and silicon was found to be the smaller effective size of C compared to Si, and the resulting lack of space around C. This was later reformulated as the ball-in-a-box[92] model (Scheme 15a), which constituted a first step on the road towards a truly pentavalent carbon.

The ball-in-a-box model[92] applies in the case of a configuration in which the central atom can move comparatively easily in the central cavity of a box constituted by five surrounding, mutually nonbonded substituents (see Scheme 15, left). The latter compete for bonding to the central atom but cannot come closer due to mutual steric (Pauli) repulsion. A silicon atom fits perfectly into the central cavity: it is large enough to bind simultaneously to all five substituents, yielding a stable, hypervalent species, such as $[Cl–\mathbf{Si}H_3–Cl]^-$. Carbon, on the other hand, is too small to simultaneously form C–Cl bonds to either axial substituent in $[Cl–\mathbf{C}H_3–Cl]^{-‡}$. Therefore, this species is a transition state: it is labile with respect to carbon moving towards one of the two axial Cl substituents, thereby forming one complete and strong C–Cl bond at the expense of sacrificing the other C–Cl bond. This process brings us to the reactant complex Cl^-CH_3Cl.

Hypervalent-carbon species $[Cl–\mathbf{C}R_3–Cl]^-$ can be formed if the $\mathbf{C}R_3$ moiety becomes internally sufficiently tightly bound and rigid, such that the central carbon atom can no longer be pulled away from the central cavity by the axial substituents, that is, when $\mathbf{C}R_3$ behaves like a rigid "disk-between-balls" (see Scheme 15, right).[93] One way to achieve this is to make the C–X bond very weak, for example, in $[Ng–CH_3–Ng]^+$ complexes, in which Ng is a noble gas atom. These cationic species are isoelectronic to $[Cl–CH_3–Cl]^{-‡}$, yet, unlike the latter, they are a stable minimum on the PES.

In 2009, Bickelhaupt and co-workers[29] provided a proof-of-concept for "freezing" a classical, anionic S_N2@C transition state, that is, for turning what is normally a labile structure into a stable hypervalent species. Unlike prior studies[94] that employed molecular scaffolds to confine the axial substituents (see, e.g., compound **C** in Scheme 16), they started instead from the transition state structure of $Cl^- + CH_3Cl$. Making use of the insight that reduced C–X bond strength and increased CR_3 rigidity, in principle, move the nature of $[Cl–CR_3–Cl]^-$ from labile TS to stable hypervalent species, they found that a heavier halogen and a CR_3 moiety involving a π-accepting substituent would be excellent features for achieving the objective. Indeed, $[I–C(CN)_3–I]$ and $[At–C(CN)_3–At]^-$ were computationally confirmed to be stable, D3 h-symmetric minima on the PES with positive asymmetric stretch vibrations and a dissociation energy of 21 kcal mol^{-1} for loss of a halide ion.[29]

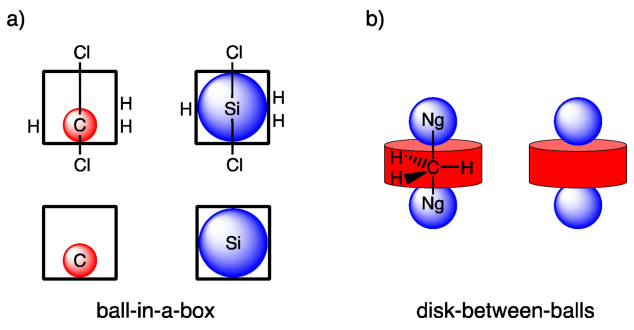

Scheme 15. Ball-in-a-box[92] (left) and disk-between-balls[93] (right) models (Ng = Noble gas element).

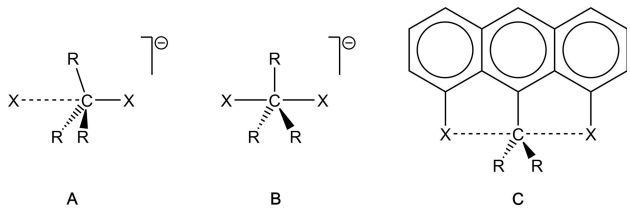

Scheme 16. Non-hypervalent (**A**) versus hypervalent (**B**) and confined (**C**) carbon.

The proof of principle shown for $[I–C(CN)_3–I^-$ has inspired the quest for hypervalent carbon in other trigonal bipyramidal configurations.[95] It was shown for $C(CN)_5^-$ that the proton affinity of the substituents R largely influences the propensity to form either a stable pentavalent species (**B** in Scheme 16) or a localized non-hypervalent species (**A** in Scheme 16).[96] At ZORA-BP86/TZ2P, the PA values are respectively[97] 372.7 kcal mol^{-1} (F^-), 333.5 kcal mol^{-1} (Cl^-), 324.3 kcal mol^{-1} (Br^-), 315.9 kcal mol^{-1} (I^-), and 313.5 kcal mol^{-1} (At^-). The cyanide ion with a PA value[64] of 349.4 kcal mol^{-1} falls in-between fluoride and chloride, and should therefore not be a stable D_{3h}-symmetric species **B**, but C_{3v}-symmetric species **A**. Frequency analysis of the optimized $C(CN)_5^-$ species indeed revealed an imaginary frequency, corresponding to a TS. On a separate, but related quest for hypervalence, Goesten and co-workers[98] found that fluoride, the smallest existing anion, was capable of coordinating to eight silicon atoms. In this case, the "box" (a key building block of large pore zeolites referred to as double-four-ring) had the perfect size to bind F^- at its center and set the scene for hypervalent bonding and significant charge transfer. This work highlights the delicate interplay between strain and hypervalent bonding, the approach having the potential for application to other solid-state compounds and beyond.

Proceeding from the ball-in-a-box[92] model, one can reverse the trends for S_N2@P[61] and S_N2@Si[62] reactions and shift the mechanism such that it proceeds over a barrier, similar to what is normally found for S_N2@C, and as opposed to the single-well PES that is more typical for third- and higher-period central atoms. Modulation of the steric interaction and thus the Pauli repulsion at the TS along the series S_N2@SiH_3Cl, S_N2@$Si(CH_3)_3Cl$, S_N2@$Si(C_2H_5)_3Cl$ and S_N2@$Si(OCH_3)_3Cl$, causes the energy profile to change from a single-well, to a triple-well, and then into a prototypical double-well PES, respectively. Increased steric bulk

around the central atom acts to block the backside approach of the incoming nucleophile. An energy decomposition analysis showed that both the strain and the Pauli repulsion increase significantly with the larger size of the ligand.[61–62,99]

6. Outlook

Bimolecular nucleophilic substitution (S_N2) reactions are fundamentally simple and ubiquitous processes that are central to a wide range of organic, biochemical, and biological transformations. In this Minireview we have seen how S_N2 reactions are extremely sensitive to the nature of the substrate, nucleophile, and leaving group. High-level quantum chemical and dynamical calculations, as well as experimental techniques, are essential for probing the reaction mechanism and associated product distributions. This Minireview highlights the complexity of S_N2 substitution and the various factors controlling the associate rate and competition with other pathways. We hope the insights into S_N2 reactivity collected herein from various pioneering studies, will serve as guidelines for new physicochemical experiments and design principles in synthesis.

Some general guidelines for understanding S_N2 reactions include: (a) stronger bases are better nucleophiles, unless an E2 pathway is accessible which benefits more from a strong base than S_N2; (b) leaving groups with a weak bond to the substrate present enhanced reactivity (C–I≫C–F); (c) increasingly electropositive central atoms result in enhanced electrophilicity and faster reactions; (d) less steric bulk around the central atom lowers reaction barriers; (e) sterically bulky substituents also drastically transform the shape of the PES, i.e., from single-well, to triple-well, and then to double-well); (f) solvation of ionic identity S_N2 reactions raises barriers and can also change the shape of the PES.

Simple models, such as the "ball-in-a-box", can easily explain the key change of mechanism in going from the second-period elements (e.g. S_N2@C) to third-period analogs (e.g. S_N2@Si) and the associated transformation of the PES, from double-well with a central TS to single-well, respectively. The steric nature of the transition state, and how this can be exploited for the reappearance of reaction barriers in the case of S_N2@P or S_N2@Si will play an important role in future studies on biologically relevant processes that involve nucleophilic attack on phosphorus, such as hydrolysis of phosphodiester bonds in GTPase, ATPase, and DNA polymerase enzymes. Moreover, the stepwise Walden-inversion on species with flexible substituents on the central atom will become an important issue for these biological processes. Lastly, the S_N2@C transition structure can be transformed into a hypervalent energy minimum with a single-well PES by modulating the substituents surrounding the carbon atom (cf. "disk-between-balls" model).

Acknowledgements

The following organizations are thanked for financial support: the Ministerio de Ciencia e Innovación (MICINN, project number CTQ2008-06532/BQU), the DIUE of the Generalitat de Catalunya (project number 2009SGR528), the Netherlands Organization for Scientific Research (NWO), the Planetary and Exo-Planetary Science program (PEPSci), and the Dutch Astrochemistry Network (DAN). The authors thank Stephanie van der Lubbe, Dr. Jörn Nitsch, Pascal Vermeeren, Dr. Lando P. Wolters, and the reviewers for helpful discussions and constructive criticism of the manuscript.

Conflict of Interest

The authors declare no conflict of interest.

Keywords: bimolecular nucleophilic substitutions (S_N2) · hypervalency · organic chemistry · potential energy surface · reaction barriers

[1] a) P. Walden, *Ber. Dtsch. Chem. Ges.* **1893**, *26*, 210; b) F. A. Carey, R. J. Sundberg, *Adv. Org. Chem.*, Plenum Press, New York, USA, **1984**; c) M. B. Smith, *March's Advanced Organic Chemistry: Reactions, Mechanisms and Structure*; 7th ed. Wiley: New York, **2013**; d) S. Shaik, H. B. Schlegel, S. Wolfe, *Theoretical Aspects of Physical Organic Chemistry: The S_N2 Reaction*, Wiley, New York, **1992**; e) J. M. Riveros, S. M. José, K. Takashima, *Adv. Phys. Org. Chem.* **1985**, *21*, 197; f) A. de Cozar, E. Ortega-Carrasco, E. San Sebastian, O. Larranaga, J.-D. Marechal, F. M. Bickelhaupt, F. P. Cossío, *ChemPhysChem* **2016**, *17*, 3932.

[2] a) S. Gronert, *Acc. Chem. Res.* **2003**, *36*, 848; b) F. M. Bickelhaupt, E. J. Baerends, N. M. M. Nibbering, T. Ziegler, *J. Am. Chem. Soc.* **1993**, *115*, 9160; c) F. M. Bickelhaupt, G. J. H. Buisman, L. J. de Koning, N. M. M. Nibbering, E. J. Baerends, *J. Am. Chem. Soc.* **1995**, *117*, 9889; d) F. M. Bickelhaupt, G. J. H. Buisman, L. J. de Koning, N. M. M. Nibbering, E. J. Baerends, *J. Am. Chem. Soc.* **1996**, *118*, 1579; e) F. M. Bickelhaupt, L. J. de Koning, N. M. M. Nibbering, *J. Phys. Org. Chem.* **1992**, *5*, 179; f) F. M. Bickelhaupt, L. J. de Koning, N. M. M. Nibbering, *Tetrahedron* **1993**, *49*, 2077.

[3] a) A. P. Bento, M. Sola, F. M. Bickelhaupt, *J. Chem. Theory Comput.* **2008**, *4*, 929; b) A. P. Bento, M. Sola, F. M. Bickelhaupt, *J. Chem. Theory Comput.* **2010**, *6*, 1445; c) M. Swart, M. Solà, F. M. Bickelhaupt, *J. Chem. Theory Comput.* **2010**, *6*, 3145.

[4] a) J. M. Gonzales, R. S. Cox III, S. T. Brown, W. D. Allen, H. F. Schaefer III, *J. Phys. Chem. A* **2001**, *105*, 11327; b) J. M. Gonzales, C. Pak, R. S. Cox, W. D. Allen, H. F. Schaefer III, A. G. Császár, G. Tarczay, *Chem. Eur. J.* **2003**, *9*, 2173; c) J. M. Gonzales, W. D. Allen, H. F. Schaefer, *J. Phys. Chem. A* **2005**, *109*, 10613; d) M. Grüning, O. Gritsenko, E. J. Baerends, *J. Phys. Chem. A* **2004**, *108*, 4459; e) M. Swart, A. W. Ehlers, K. Lammertsma, *Mol. Phys.* **2004**, *102*, 2467; f) M. Swart, M. Sola, F. M. Bickelhaupt, *J. Comput. Chem.* **2007**, *28*, 1551; g) C. Acosta-Silva, V. Branchadell, *J. Phys. Chem. A* **2007**, *111*, 12019; h) E. Westphal, J. R. Pliego, *J. Phys. Chem. A* **2007**, *111*, 10068; i) Y. Zhao, D. G. Truhlar, *J. Chem. Theory Comput.* **2010**, *6*, 1104; j) M. Swart, F. M. Bickelhaupt, *Molecules* **2013**, *18*, 7726; k) R. Sun, C. J. Davda, J. Zhang, W. L. Hase, *Phys. Chem. Chem. Phys.* **2015**, *17*, 2589; l) I. Szabó, G. Czakó, *J. Phys. Chem. A* **2017**, *121*, 5748; m) B. Hajdu, G. Czakó, *J. Phys. Chem. A* **2018**, *122*, 1886.

[5] T. B. Phan, C. Nolte, S. Kobayashi, A. R. Ofial, H. Mayr, *J. Am. Chem. Soc.* **2009**, *131*, 11392.

[6] P. R. Rablen, B. D. McLarney, B. J. Karlow, J. E. Schneider, *J. Org. Chem.* **2014**, *79*, 867.

[7] L. P. Wolters, Y. Ren, F. M. Bickelhaupt, *ChemistryOpen* **2014**, *3*, 29.

[8] a) F. M. Bickelhaupt, *J. Comput. Chem.* **1999**, *20*, 114; b) D. H. Ess, K. N. Houk, *J. Am. Chem. Soc.* **2007**, *129*, 10646; c) D. H. Ess, G. O. Jones, K. N. Houk, *Org. Lett.* **2008**, *10*, 1633; d) D. H. Ess, K. N. Houk, *J. Am. Chem.*

Soc. **2008**, *130*, 10187; e) W.-J van Zeist, F. M. Bickelhaupt, *Org. Biomol. Chem.* **2010**, *8*, 3118; f) I. Fernández, F. M. Bickelhaupt, *Chem. Soc. Rev.* **2014**, *43*, 4953; g) L. P. Wolters, F. M. Bickelhaupt, *WIREs Comput. Mol. Sci.* **2015**, *5*, 324; h) F. M. Bickelhaupt, K. N. Houk, *Angew. Chem. Int. Ed.* **2017**, *56*, 10070; *Angew. Chem.* **2017**, *129*, 10204.

[9] a) J. M. Garver, Y. R. Fang, N. Eyet, S. M. Villano, V. M. Bierbaum, K. C. Westaway, *J. Am. Chem. Soc.* **2010**, *132*, 3808; b) M. A. van Bochove, F. M. Bickelhaupt, *Eur. J. Org. Chem.* **2008**, *649*; c) X. Chen, J. I. Brauman, *J. Am. Chem. Soc.* **2008**, *130*, 15038; d) F. M. Bickelhaupt, E. J. Baerends, N. M. M. Nibbering, *Chem. Eur. J.* **1996**, *2*, 196.

[10] a) N. Menshutkin, *Z. Phys. Chem.* **1890**, *5*, 589; b) N. Menshutkin, *Z. Phys. Chem.* **1890**, *6*, 41.

[11] a) M. Sola, A. Lledós, M. Duran, J. Bertrán, J.-L. M. Abboud, *J. Am. Chem. Soc.* **1991**, *113*, 2873; b) H. Castejon, K. B. Wiberg, *J. Am. Chem. Soc.* **1999**, *121*, 2139.

[12] a) D. K. Bohme, G. I. Mackay, *J. Am. Chem. Soc.* **1981**, *103*, 978; b) D. K. Bohm, A. B. Raksit, *J. Am. Chem. Soc.* **1984**, *106*, 3447.

[13] a) K. Ohta, K. Morokuma, *J. Phys. Chem.* **1985**, *89*, 5845; b) S. C. Tucker, D. G. Truhlar, *J. Am. Chem. Soc.* **1990**, *112*, 3347.

[14] a) J. Zhang, L. Yang, J. Xie, W. L. Hase, *J. Phys. Chem. Lett.* **2016**, *7*, 660; b) J. Xie, M. J. Scott, W. L. Hase, P. M. Hierl, A. A. Viggiano, *Z. Phys. Chem.* **2015**, *229*, 1747.

[15] a) J. Xie, R. Otto, R. Wester, W. L. Hase, *J. Chem. Phys.* **2015**, *142*, 244308; b) R. Sun, J. Xie, J. Zhang, W. L. Hase, *Int. J. Mass Spectrom.* **2015**, *377*, 222; c) X. Liu, J. Xie, J. Zhang, L. Yang, W. L. Hase, *J. Phys. Chem. Lett.* **2017**, *8*, 1885.

[16] a) D. K. Bohme, A. B. Raksit, *Can. J. Chem.* **1985**, *63*, 3007; b) C. K. Regan, S. L. Craig, J. I Brauman, *Science* **2002**, *295*, 2245.

[17] a) H. Tachikawa, *J. Chem. Phys.* **2006**, *125*, 133119; b) R. Otto, J. Brox, S. Trippel, M. Stei, T. Best, R. Wester, *Nat. Chem.* **2012**, *4*, 534; c) D. L. Thomsen, J. N. Reece, C. M. Nichols, S. Hammerum, V. M. Bierbaum, *J. Am. Chem. Soc.* **2013**, *135*, 15508.

[18] M. J. Ryding, A. Debnárová, I. Fernández, E. Uggerud, *J. Org. Chem.* **2015**, *80*, 6133.

[19] T. A. Hamlin, B. van Beek, L. P. Wolters, F. M. Bickelhaupt, *Chem. Eur. J.* **2018**, *24*, DOI: 10.1002/chem.201706075.

[20] a) S. R. Vande Linde, W. L. Hase, *J. Am. Chem. Soc.* **1989**, *111*, 2349; b) S. R. Vande Linde, W. L. Hase, *J. Chem. Phys.* **1990**, *93*, 7962.

[21] A. A. Viggiano, R. A. Morris, J. S. Pschkewitz, J. F. Paulson, *J. Am. Chem. Soc.* **1992**, *114*, 10477.

[22] a) L. Sun, K. Song, W. L. Hase, *Science* **2002**, *296*, 875; b) P. Manikandan, J. Zhang, W. L. Hase, *J. Phys. Chem. A* **2012**, *116*, 3061.

[23] a) M. Stei, E. Carrascosa, M. A. Kainz, A. H. Kelkar, J. Meyer, I. Szabó, R. Wester, *Nat. Chem.* **2016**, *8*, 151; b) J. Mikosch, S. Trippel, C. Eichhorn, R. Otto, U. Lourderaj, J. X. Zhang, W. L. Hase, M. Weidemuller, R. Wester, *Science* **2008**, *319*, 183.

[24] C. Hennig, S. Schmatz, *J. Chem. Phys.* **2009**, *131*, 224303.

[25] E. Carrascosa, J. Meyer, J. Zhang, M. Stei, T. Michaelsen, W. L. Hase, L. Yang, R. Wester, *Nat. Commun.* **2017**, *8*, 25.

[26] J. Xie, R. Sun, M. R. Siebert, R. Otto, R. Wester, W. L. Hase, *J. Phys. Chem. A* **2013**, *117*, 7162.

[27] a) I. Szabó, F. Czakó, *Nat. Commun.* **2014**, *6*, 5972; b) Y.-T. Ma, X. Ma, A. Li, H. Guo, L. Yang, J. Zhang, W. L. Hase, *Phys. Chem. Chem. Phys.* **2017**, *19*, 20127.

[28] J. Xie, W. L. Hase, *Science* **2016**, *352*, 32.

[29] S. Pierrefixe, S. J. M. van Stralen, J. N. P. van Stralen, C. Fonseca Guerra, F. M. Bickelhaupt, *Angew. Chem. Int. Ed.* **2009**, *48*, 6469.

[30] a) S. Gronert, S. R. Kass, *J. Org. Chem.* **1997**, *62*, 7991; b) G. N. Merrill, S. Gronert, S. R. Kass, *J. Phys. Chem. A* **1997**, *101*, 208; c) A. P. Bento, F. M. Bickelhaupt, *J. Org. Chem.* **2008**, *73*, 7290; d) R. D. Bach, A. G. Baboul, H. B. Schlegel, *J. Am. Chem. Soc.* **2001**, *123*, 5787; e) J. Zhang, U. Lourderaj, S. V. Addepalli, W. A. de Jong, W. L. Hase, *J. Phys. Chem. A* **2009**, *113*, 1976; f) J. X. Zhang, W. L. Hase, *J. Phys. Chem. A* **2010**, *114*, 9635; g) I. Szabó, A. G. Császár, G. Czakó, *Chem. Sci.* **2013**, *4*, 4362; h) G. Czakó, J. M. Bowman, *J. Phys. Chem. A* **2014**, *118*, 2839; i) I. Szabó, G. Czakó, *J. Phys. Chem. A* **2015**, *119*, 3134; j) I. Szabó, G. Czakó, *J. Phys. Chem. A* **2017**, *121*, 9005; k) I. Alkorta, J. C. R. Thacker, P. L. A. Popelier, *J. Comput. Chem.* **2018**, *39*, 546.

[31] R. R. Sauers, *J. Chem. Theory Comput.* **2010**, *6*, 602.

[32] E. Uggerud, *Chem. Eur. J.* **2006**, *12*, 1127.

[33] L. G. Arnaut, S. J. Formosinho, *Chem. Eur. J.* **2007**, *13*, 8018.

[34] C.-H. Wu, B. Galabov, J. I.-C. Wu, S. Ilieva, P. von R. Schleyer, *J. Am. Chem. Soc.* **2014**, *136*, 3118.

[35] a) I. Erden, S. Gronert, J. R. Keeffe, J. Ma, N. Ocal, C. Gärtner, L. L. Soukup, *J. Org. Chem.* **2014**, *79*, 6410; b) R. Robiette, T. Trieu-Van, V. K. Aggarwal, J. B. Harvey, *J. Am. Chem. Soc.* **2016**, *138*, 734.

[36] a) K. Takashima, J. M. Riveros, *J. Am. Chem. Soc.* **1977**, *100*, 6128; b) G. Occhiucci, M. Speranza, L. J. de Koning, N. M. M. Nibbering, *J. Am. Chem. Soc.* **1989**, *111*, 7387; c) J. R. Pliego, Jr., J. M. Riveros, *Chem. Eur. J.* **2001**, *7*, 169; d) J. R. Pliego, Jr., J. M. Riveros, *J. Phys. Chem. A* **2002**, *106*, 371; e) H. Tachikawa, M. Igarashi, T. Ishibashi, *J. Phys. Chem. A* **2002**, *106*, 10977; f) C. Acosta-Silva, V. Branchadell, *J. Phys. Chem. A* **2007**, *111*, 12019; g) R. Valero, L. Song, J. Gao, D. G. Truhlar, *J. Chem. Theory Comput.* **2009**, *5*, 1; h) T. C. Correra, J. M. Riveros, *J. Phys. Chem. A* **2010**, *114*, 11910; i) R. Kretschmer, M. Schlangen, H. Schwarz, *Angew. Chem. Int. Ed.* **2011**, *50*, 5387; j) S. Itoh, N. Yoshimura, M. Sato, H. Yamataka, *J. Org. Chem.* **2011**, *76*, 8294; k) R. Kretschmer, M. Schlangen, M. Kaupp, H. Schwarz, *Organometallics* **2012**, *31*, 3816; l) J. Zhang, Y. Xu, J. Chen, D. Wang, *Phys. Chem. Chem. Phys.* **2014**, *16*, 7611; m) Y. Xu, J. Zhang, D. Wang, *J. Chem. Phys.* **2015**, *142*, 244505; n) S.-S. Lee, V. H. Jadhav, J.-Y. Kim, J.-H. Chun, A. Lee, S.-Y. Kim, S. Lee, D. W. Kim, *Tetrahedron* **2015**, *71*, 2863; o) J. Liang, Q. Su, Y. Wang, Z. Geng, *Bull. Chem. Soc. Jpn.* **2015**, *88*, 110; p) Y. G. Proenza, M. A. F. de Souza, R. L. Longo, *Chem. Eur. J.* **2016**, *22*, 16220.

[37] X. P. Wu, X. M. Sun, X. G. Wei, Y. Ren, N. B. Wong, W. K. Li, *J. Chem. Theory Comput.* **2009**, *5*, 1597.

[38] Y. Ren, H. Yamataka, *Chem. Eur. J.* **2007**, *13*, 677.

[39] J. O. Edwards, R. G. Pearson, *J. Am. Chem. Soc.* **1962**, *84*, 16.

[40] S. M. Villano, N. Eyet, W. C. Lineberger, V. M. Bierbaum, *J. Am. Chem. Soc.* **2009**, *131*, 8227.

[41] J. M. Garver, S. Gronert, V. M. Bierbaum, *J. Am. Chem. Soc.* **2011**, *133*, 13894.

[42] a) S. J. Hoz, *J. Org. Chem.* **1982**, *47*, 3545; b) J. D. Evanseck, J. F. Blake, W. L. Jorgensen, *J. Am. Chem. Soc.* **1987**, *109*, 2349; c) E. Buncel, I.-H. Um, *Tetrahedron* **2004**, *60*, 7801; d) Y. Ren, H. Yamataka, *J. Org. Chem.* **2007**, *72*, 5660; e) A. M. McAnoy, M. R. L. Paine, S. J. Blanksby, *Org. Biomol. Chem.* **2008**, *6*, 2316; f) I.-H. Um, L.-R. Im, E. Buncel, *J. Org. Chem.* **2010**, *75*, 8571; g) X.-G. Wie, X.-M. Sun, X.-P. Wu, Y. Ren, N.-B. Wong, W.-K. Li, *J. Org. Chem.* **2010**, *75*, 4212; h) I.-H. Um, J.-S. Kang, M.-Y. Kim, E. Buncel, *J. Org. Chem.* **2013**, *78*, 8689; i) Y. Ren, X.-G. Wie, S.-J. Ren, K.-C. Lau, N.-B. Wong, W.-K. Li, *J. Comput. Chem.* **2013**, *34*, 1997.

[43] a) J. C. Marie, C. Courillon, M. Malacria, *Eur. J. Org. Chem.* **2006**, *463*; b) D. G. Gai, Y. Ren, *Int. J. Quantum Chem.* **2007**, *107*, 1487; c) A. Ebrahimi, M. Habibi, A. Amirmijani, *J. Mol. Struct.* **2007**, *809*, 115; d) Y. Ren, X. Wang, S. Y. Chu, N. B. Wong, *Theor. Chem. Acc.* **2008**, *119*, 407; e) Y. Ren, J. G. Gai, Y. Xiong, K. H. Lee, S. Y. Chu, *J. Phys. Chem. A* **2007**, *111*, 6615; f) Q.-G. Li, K. Xu, Y. Ren, *J. Phys. Chem. A* **2015**, *119*, 3878; g) J. Z. A. Laloo, L. Rhyman, P. Ramasami, F. M. Bickelhaupt, A. de Cózar, *Chem. Eur. J.* **2016**, *22*, 4431; h) J. Z. A. Laloo, L. Rhyman, O. Larranaga, P. Ramasami, F. M. Bickelhaupt, A. de Cozar, *Chem. Asian J.* **2018**, *13*, DOI: 10.1002/asia.201800082.

[44] a) Q. Li, Y. Xue, *J. Phys. Chem. A* **2009**, *113*, 10359; b) M. Breugst, H. Mayr, *J. Am. Chem. Soc.* **2010**, *132*, 15380; c) M. Breugst, F. C. Bautista, H. Mayr, *Chem. Eur. J.* **2012**, *18*, 127; d) P. A. Byrne, K. Karaghiosoff, H. Mayr, *J. Am. Chem. Soc.* **2016**, *138*, 11272; e) A. Schade, I. Tchernook, M. Bauer, A. Oehlke, M. Breugst, J. Friedrich, S. Spange, *J. Org. Chem.* **2017**, *82*, 8476.

[45] L. Brinchi, R. Germani, G. Savelli, N. Spreti, *Eur. J. Org. Chem.* **2006**, 4270.

[46] K. C. Westaway, Y. R. Fang, S. MacMillar, O. Matsson, R. A. Poirier, S. M. Islam, *J. Phys. Chem. A* **2008**, *112*, 10264.

[47] P. J. Ji, J. H. Atherton, M. I. Page, *Faraday Discuss.* **2010**, *145*, 15.

[48] R. D. Bach, O. Dmitrenko, C. Thorpe, *J. Org. Chem.* **2008**, *73*, 12.

[49] O. Dmitrenko, C. Thorpe, R. D. Bach, *J. Org. Chem.* **2007**, *72*, 8298.

[50] a) S. M. Bachrach, D. C. Mulhearn, *J. Phys. Chem.* **1996**, *100*, 3535; b) S. M. Bachrach, A. C. Chamberlin, *J. Org. Chem.* **2003**, *68*, 4743.

[51] A. Mahmood, E. S. Teixeira, R. L. Longo, *J. Org. Chem.* **2015**, *80*, 8198.

[52] X. Hao, Z. Xu, H. Lu, X. Dai, T. Yang, X. Lin, F. Ren, *Org. Lett.* **2015**, *17*, 3382.

[53] a) F. J. Schmitz, S. K. Agarwal, S. P. Gunasekera, P. G. Schmidt, J. N. Shoolery, *J. Am. Chem. Soc.* **1983**, *105*, 4835; b) M. E. Wall, M. C. Wani, C. E. Cook. K. N. Palmer, A. T. McPhall, G. A. Sim, *J. Am. Chem. Soc.* **1966**, *88*, 3888.

[54] R. R. Holmes, *Chem. Rev.* **1990**, *90*, 17.

[55] C. Chuit, R. J. P. Corriu, C. Reye, J. C. Young, *Chem. Rev.* **1993**, *93*, 1371.

[56] R. Damrauer, J. A. Hankin, *Chem. Rev.* **1995**, *95*, 1137.

[57] A. P. Bento, M. Sola, F. M. Bickelhaupt, *J. Comput. Chem.* **2005**, *26*, 1497.

[58] a) E. van Lenthe, E. J. Baerends, J. G. Snijders, *J. Chem. Phys.* **1993**, *99*, 4597; b) G. te Velde, F. M. Bickelhaupt, E. J. Baerends, C. Fonseca Guerra,

S. J. A. van Gisbergen, J. G. Snijders, T. Ziegler, *J. Comput. Chem.* **2001**, *22*, 931.
[59] M. Swart, F. M. Bickelhaupt, *J. Comput. Chem.* **2008**, *29*, 724.
[60] S. Osuna, M. Swart, M. Solà, *J. Am. Chem. Soc.* **2009**, *131*, 129.
[61] M. A. van Bochove, M. Swart, F. M. Bickelhaupt, *J. Am. Chem. Soc.* **2006**, *128*, 10738.
[62] A. P. Bento, F. M. Bickelhaupt, *J. Org. Chem.* **2007**, *72*, 2201.
[63] A. P. Bento, F. M. Bickelhaupt, *Chem. Asian J.* **2008**, *3*, 1783.
[64] O. I. Kolodiazhnyi, A. Kolodiazhna, *Tetrahedron: Asymmetry* **2017**, *28* 1651.
[65] R. R. Holmes, *Chem. Rev.* **1996**, *96*, 927.
[66] C. Y. Wong, D. K. Kennepohl, R. G. Cavell, *Chem. Rev.* **1996**, *96*, 1917.
[67] M. A. van Bochove, M. Swart, F. M. Bickelhaupt, *ChemPhysChem* **2007**, *8*, 2452.
[68] M. A. van Bochove, M. Swart, F. M. Bickelhaupt, *Phys. Chem. Chem. Phys.* **2009**, *11*, 259.
[69] M. A. van Bochove, G. Roos, C. Fonseca Guerra, T. A. Hamlin, F. M. Bickelhaupt, *Chem. Commun.* **2018**, *54*, 3448.
[70] a) T. Nakamura, Y. Zhao, Y. Yamagata, Y. J. Hua, W. Yang, *Nature* **2012**, *487*, 196; b) E. M. De La Cruz, E. M. Ostap, *Methods Enzymol.* **2009**, *455*, 157; c) A. J. Berdis, *Chem. Rev.* **2009**, *109*, 2862; d) W. W. Cleland, A. C. Hengge, *Chem. Rev.* **2006**, *106*, 3252.
[71] C. Lad, N. H. Williams, R. Wolfenden, *Proc. Natl. Acad. Sci. USA* **2003**, *100*, 5607.
[72] N. Ashkenazi, Y. Segall, R. Chen, G. Sod-Moriah, E. Fattal, *J. Org. Chem.* **2010**, *75*, 1917.
[73] M. K. Kesharwani, M. A. S. Khan, T. Bandyopadhyay, B. Ganguly, *Theor. Chem. Acc.* **2010**, *127*, 39.
[74] a) S. M. Bachrach, J. T. Woody, D. C. Mulhearn, *J. Org. Chem.* **2002**, *67*, 8983; b) J. M. Hayes, S. M. Bachrach, *J. Phys. Chem. A* **2003**, *107*, 7952; c) P. A. Fernandes, M. J. Ramos, *Chem. Eur. J.* **2004**, *10*, 257; d) Y. Ren, J.-G. Fai, Y. Xiong, K.-H. Lee, S.-Y. Chu, *J. Phys. Chem. A* **2007**, *111*, 6615; e) D. D. Sung, T. J. Kim, I. Lee, *J. Phys. Chem. A* **2009**, *113*, 7073; f) M. P. Sherman, W. R. Grither, R. D. McCulla, *J. Org. Chem.* **2010**, *75*, 4014; g) M. Paranjothy, M. R. Siebert, W. L. Hase, S. M. Bachrach, *J. Phys. Chem. A* **2012**, *116*, 11492; h) R. F. Höckendorf, Q. Hao, Z. Sun, B. S. Fox-Beyer, Y. Cao, O. Petru Balaj, V. E. Bondybey, C.-K. Siu, M. K. Beyer, *J. Phys. Chem. A* **2012**, *116*, 3824; i) R. P. P. Neves, P. A. Fernandes, A. J. C. Varandas, M. J. Ramos, *J. Chem. Theory Comput.* **2014**, *10*, 4842; j) M. Bortoli, L. P. Wolters, L. Orian, F. M. Bickelhaupt, *J. Chem. Theory Comput.* **2016**, *12*, 2752; k) S. A. Suarez, M. Muñoz, L. Alvarez, M. F. Venânclo, W. R. Rocha, D. E. Bikiel, M. A. Marti, F. Doctorovich, *J. Am. Chem. Soc.* **2017**, *139*, 14483.
[75] A. T. P. Carvalho, M. Swart, J. N. P. van Stralen, P. A. Fernandes, M. J. Ramos, F. M. Bickelhaupt, *J. Phys. Chem. B* **2008**, *112*, 2511.
[76] E. H. Krenske, W. A. Pryor, K. N. Houk, *J. Org. Chem.* **2009**, *74*, 5356.
[77] C. E. Paulsen, K. S. Carroll, *Chem. Rev.* **2013**, *113*, 4633.
[78] S. H. Norton, S. M. Bachrach, J. M. Hayes, *J. Org. Chem.* **2005**, *70*, 5896.
[79] A. T. P. Carvalho, P. A. Fernandes, M. Swart, J. N. P. van Stralen, F. M. Bickelhaupt, M. J. Ramos, *J. Comput. Chem.* **2009**, *30*, 710.
[80] S. Garcia-Manyes, J. Liang, R. Szoszkiewicz, T. L. Kuo, J. M. Fernandez, *Nat. Chem.* **2009**, *1*, 236.
[81] P. Dopieralski, J. Ribas-Arino, P. Anjukandi, M. Krupicka, J. Kiss, D. Marx, *Nat. Chem.* **2013**, *5*, 685.
[82] X. Chen, C. K. Regan, S. L. Craig, E. H. Krenske, K. N. Houk, W. L. Jorgensen, J. I. Brauman, *J. Am. Chem. Soc.* **2009**, *131*, 16162.
[83] G. Vayner, K. N. Houk, W. L. Jorgensen, J. I. Brauman, *J. Am. Chem. Soc.* **2004**, *126*, 9054.
[84] E. V. Jennings, K. Nikitin, Y. Ortin, D. G. Gilheany, *J. Am. Chem. Soc.* **2014**, *136*, 16217.
[85] K. Nikitin, E. V. Jennings, S. A. Sulaimi, Y. Ortin, D. G. Gilheany, *Angew. Chem. Int. Ed.* **2017**, *57*, 1480.
[86] B. Galabov, V. Nikolova, J. J. Wilke, H. F. Schaefer, W. D. Allen, *J. Am. Chem. Soc.* **2008**, *130*, 9887.
[87] H. D. Banks, *J. Org. Chem.* **2008**, *73*, 2510.
[88] S. M. Bachrach, C. J. Walker, F. Lee, S. Royce, *J. Org. Chem.* **2007**, *72*, 5174.
[89] S. B. Liu, H. Hu, L. G. Pederset, *J. Phys. Chem. A* **2010**, *114*, 5913.
[90] a) A. E. Flores, S. Gronert, *J. Am. Chem. Soc.* **1999**, *121*, 2627; b) S. Gronert, L. M. Pratt, S. Mogali, *J. Am. Chem. Soc.* **2001**, *123*, 3081.
[91] S. Pierrefixe, F. M. Bickelhaupt, *Struct. Chem.* **2007**, *18*, 813.
[92] S. Pierrefixe, C. Fonseca Guerra, F. M. Bickelhaupt, *Chem. Eur. J.* **2008**, *14*, 819.
[93] S. C. A. H. Pierrefixe, J. Poater, C. Im, F. M. Bickelhaupt, *Chem. Eur. J.* **2008**, *14*, 6901.
[94] a) T. R. Forbus Jr, J. C. Martin, *J. Am. Chem. Soc.* **1979**, 101, 5057; b) J. C. Martin, *Science* **1983**, *221*, 509; c) F. Scherbaum, A. Grohmann, G. Müller, H. Schmidbaur, *Angew. Chem. Int. Ed.* **1989**, *28*, 463; d) K.-Y. Akiba, M. Yamashita, Y. Yamamoto, S. Nagase, *J. Am. Chem. Soc.* **1999**, *121*, 10644; e) M. Yamashita, Y. Yamamoto, K.-Y. Akiba, D. Hashizume, F. Iwasaki, N. Takagi, S. Nagase, *J. Am. Chem. Soc.* **2005**, *127*, 4354; f) T. Yamaguchi, Y. Yamamoto, D. Kinoshita, K. Y. Akiba, Y. Zhang, C. A. Reed, D. Hashizume, F. Iwasaki, *J. Am. Chem. Soc.* **2008**, *130*, 6894; g) F.-C. Liu, H.-G. Chen, G.-H. Lee, *Organometallics* **2014**, *34*, 42.
[95] a) Y.-B. Wu, Y.-Q. Li, H. Bai, H.-G. Lu, S.-D. Li, H.-J. Zhai, Z.-X. Wang, *J. Chem. Phys.* **2014**, *140*, 104302; b) W. C. McKee, J. Agarwal, H. F. Schaefer III, P. von R. Schleyer, *Angew. Chem. Int. Ed.* **2014**, *53*, 7875
[96] F. M. Bickelhaupt, C. Fonseca Guerra, N. S. Zefirov, *Mendeleev Commun.* **2010**, *20*, 72.
[97] M. Swart, F. M. Bickelhaupt, *J. Chem. Theory Comput.* **2006**, *2*, 281.
[98] M. G. Goesten, R. Hoffman, F. M. Bickelhaupt, E. J. M. Hensen, *Proc. Natl. Acad. Sci. USA* **2017**, *114*, 828.
[99] a) W. J. van Zeist, F. M. Bickelhaupt, *Chem. Eur. J.* **2010**, *16*, 5538. See also: b) I. Fernandez, G. Frenking, E. Uggerud, *Chem. Eur. J.* **2009**, *15*, 2166. c) I. Fernandez, G. Frenking, E. Uggerud, *Chem. Eur. J.* **2010**, *16*, 5542.

Manuscript received: December 21, 2017
Version of record online: April 19, 2018